

Settlement Due to Circular Load on Finite Two-Layered Soil System

Yugandhar Damalla

A Dissertation Submitted to
Indian Institute of Technology Hyderabad
In Partial Fulfillment of the Requirements for
The Degree of Master of Technology



भारतीय प्रौद्योगिकी संस्थान हैदराबाद
Indian Institute of Technology Hyderabad

Department of Civil Engineering

June, 2012

Declaration

I declare that this written submission represents my ideas in my own words, and where other's ideas or words have been included, I have adequately cited and referenced the original sources. I also declare that I have adhered to all principles of academic honesty and integrity and have not misrepresented or fabricated or falsified any idea/data/fact/source in my submission. I understand that any violation of the above will be a cause for disciplinary action by the Institute and can also evoke penal action from the sources that have thus not been properly cited, or from whom proper permission has not been taken when needed.

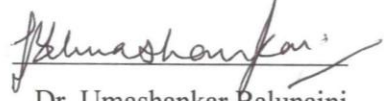


Yugandhar Damalla

Ce10m08

Approval Sheet

This thesis entitled "*Settlement due to Circular Load on Finite Two- Layered Soil System*" by **Yugandhar Damalla** is approved for the degree of Master of Technology from IIT Hyderabad.



Dr. Umashankar Balunaini

Advisor



Dr. Sireesh Saride

Examiner



Dr. B. Venkatesham

Chairman

Acknowledgements

I would like to express my deep gratitude to my supervisor Dr. Umashankar Baluanaini for his involvement and encouragement throughout this thesis work. I am greatly indebted to him for his unwavering commitment, thought provoking and constructive comments to improve my work. His approach to a research problem, time management had really impressed me. I shall sincerely try to instill the same in my life. I consider myself fortunate to have him as my supervisor.

I would like to thank Dr. S. Sireesh, Prof. K.V.L. Subramaniam, Dr. A. Rajagopal for their encouragement and support during my course work of Infrastructural systems.

I thank to my classmates Jancy, Sahith, Mahesh, Harish, Mahendra, Faraz and all civil Eng. Department students of M.Tech. and Ph.D. for making my stay at IITH memorable in my life and convey my best wishes to them.

Lastly, I convey my beloved love to my parents and family members for their encouragement and support for bringing me to this stage.

Thank you very much.

Dedicated to

My family and friends

Abstract

Structures are commonly founded on layered soil deposits. Many instances are there where the soil profile consisted of two-layer soil deposit, underlain by a rock stratum. So in this thesis, finite two-layered soil profile overlying a stiff soil deposit is considered. Top layer of the soil is loose sand and bottom layer of the soil is sandy gravel considered and vice versa. Elastic settlements due to a flexible and rigid circular load on a two-layer soil system without reinforcement and with incorporating reinforcement overlying a rock stratum or a stiff soil deposit are estimated by design charts and tables. As soil behavior is not elastic in nature, so approximating the soil behavior in general by elasto-plastic behavior, it is obtained by Mohr-Coulomb model in Plaxis 2D. Plastic settlements due to a flexible and rigid circular load on a two-layer soil system overlying a rock stratum or a stiff soil deposit are estimated by design charts and tables.

Nomenclature

a	Radius of the circular load
B	Diameter of the circular load
C	Cohesion of soil
E	Young's modulus
E'_{avg}	Drained average Young's modulus
E'	Drained Young's modulus
E_2	Young's modulus of bottom layer
I_p	Displacement influence factor
h	Depth of the homogenous finite layer
H_1	Top layer thickness
H_2	Bottom layer thickness
P_{av}	Average applied pressure
q	Uniformly distributed load
ρ_z	Settlement
Φ	Friction angle of soil
Ψ	Dilatancy angle of soil
ν	Poisson's ratio
σ	Normal Stress
ϵ	Normal strain
ρ/B	Ratio of Displacement to the Diameter of the circular load

Contents

Declaration.....	ii
Approval Sheet	iii
Acknowledgements.....	iv
Abstract.....	vi
Nomenclature	vii
List of Tables	x
List of Figures	xi
1 Introduction	1
1.1 Difference in behavior of load acting on flexible and rigid footing	2
1.2 Problem statement	3
1.3 Organization of the study.....	4
2 Literature review	5
2.1 Elastic solutions for Homogenous finite layer.....	5
2.2 Elastic solutions for Homogenous semi-infinite soil	6
2.3 Elastic solutions for two-layered soil system (top layer is finite and bottom layer is semi-infinite).....	7
2.4 Elastic solution for Multi-layer soil system.....	8
3 Settlement of Finite Two-layer System using Linear Stress-Strain Behavior .10	
3.1 Load on Flexible Footing.....	10
3.1.1 Elastic Solution.....	10
3.1.2 Finite Element Analysis	13
3.1.3 Results	13
3.1.4. Case Study and Validation	21
3.2 Load on a Rigid footing	24
3.2.1 Elastic solution	24
3.2.2 Finite element solution	24
4 Load-settlement response of finite two-layer system using Mohr-Coulomb model	27
4.1 Load on a Flexible footing.....	28
4.2 Load on a Rigid footing	30

5 Conclusions	34
5.1 Elastic analysis due to flexible load on finite two-layer system.....	34
5.1.1 Bottom layer is stiffer than the top layer	34
5.1.2 Top layer is stiffer than the bottom layer	34
5.2 Elastic analysis due to rigid load on finite two-layer system.....	35
5.3 Nonlinear analysis due to flexible load on finite two-layer system.....	35
5.4 Nonlinear analysis due to rigid load on finite two-layer system	35
References.....	36

List of Tables

3.1	I_ρ values for $E_1/E_2 > 1.0$ using finite element solution	19
3.2	I_ρ values for $E_1/E_2 > 1.0$ using finite element solution	20
3.3	Comparison of I_ρ values from Ueshita and Meyerhof (1967) and from the present study	22

List of Figures

1.1	Soil profile showing a finite two-layer soil system at (a) Hong Kong [Zhang and Dasaka (2010)] and (b) southern part of Bangalore (Anbazghan and Sitharam [2004])	2
1.2	Differences in behavior between flexible and rigid footings over clayey soil.....	3
1.3	Definition sketch	4
2.1	Influence factors for the vertical displacement of rigid circle (Poulos [1968a]) .	5
2.2	Vertical deflection due to circular loading for Poisson's ratio equal to 0.5 (Foster and Ahlvin)	6
2.3	Vertical surface deflections for two-layered systems for $\nu_1=\nu_2= 0.5$ (After Burmister[1943]).....	7
2.4	Equivalent modulus E_e of two-layered systems for $\nu_1=\nu_2= 0.5$ (Ueshita and Meyerhof [1967]).....	8
2.5	Approximate displacement factors for layered systems for $\nu_1=\nu_2= 0.5$ (Vesic[1963]).....	9
3.1	Displacement factors for layered systems for load on flexible footing (modified after Vesic [1963])	11
3.2	Comparison of vertical stress contours for $q=500$ kPa and $a=1$ m for [a]uniform elastic medium (constant E), $\nu=0.5$, and [b] two-layer system with $H_1=1$ m, $E_1=1$ MPa, $\nu_1=0.5$; $H_2=5$ m, $E_2=10$ MPa, $\nu_2=0.5$	12
3.3	Comparison of vertical stress contours for $q= 500$ kPa and $a=1$ m for [a] uniform elastic medium (constant E), $\nu=0.5$, and [b] two-layer system with $H_1=1$ m, $E_1=10$ MPa, $\nu_1=0.5$; $H_2=5$ m, $E_2=1$ MPa, $\nu_2=0$	12
3.4	Finite element modeling: (a) meshing, and (b) 15-noded triangular element used for discretization	13
3.5	Variation of I_p with H_1/a from elastic and finite element solutions for $\nu_1=\nu_2=0.35$, $E_1/E_2=0.01-1.0$ and corresponding to (a) $H_2/a=1.0$ and (b) $H_2/a=4.0$	15
3.6	Variation of I_p with H_1/a from elastic and finite element solutions for $\nu_1=\nu_2=0.35$, $E_1/E_2=0.01-1.0$ and corresponding to (a) $H_1/a=0.5$ and (b) $H_1/a=2.0$	16
3.7	Variation of I_p with H_1/a from elastic and finite element solutions for $\nu_1=\nu_2=0.5$, $E_1/E_2=2-100$ and corresponding to (a) $H_2/a=1.0$ and (b) $H_2/a=4.0$	17
3.8	Variation of I_p with H_1/a from elastic and finite element solutions for $\nu_1=\nu_2=0.5$, $E_1/E_2=2-100$ and corresponding to (a) $H_1/a=0.5$ and (b) $H_1/a=2.0$	18
3.9	Soil profile with the variation of E' with depth at Savings Bank Building in the City of Adelaide, South Australia (Kay and Cavagnaro, [1983]).....	23

3.10	Displacement factors for layered systems for load on rigid footing (modified after Vesic [1963]).....	24
3.11	Variation of I_p with H_1/a from Finite element solutions for $\nu_1=\nu_2=0.35$, $E_1/E_2=2-100$	26
3.12	Comparison of flexible footing (Ff) and rigid footing (Rf) for variation of I_p with H_1/a from finite element solutions for $\nu_1=\nu_2=0.35$, $E_1/E_2=2-100$, $H_2/a=4$	26
4.1	Elastic perfectly plastic behavior of soil under external load	27
4.2	Mohr-Coulomb model for load on finite two-layered soil profile	28
4.3	Variation of I_p with H_1/a from Finite element solutions for $\nu_1=\nu_2=0.35$, $E_1=2000kPa$, $E_2=1000kPa$	29
4.4	Variation of I_p with H_1/a from Finite element solutions for $\nu_1=\nu_2=0.35$, $E_2=1000 kPa$, $E_1=2000 kPa$, $5000 kPa$, $20000 kPa$ respectively corresponding to $H_2/a=1$	31
4.5	Variation of I_p with H_1/a from Finite element solutions for $\nu_1=\nu_2=0.35$, $E_2=1000 kPa$, $E_1=2000 kPa$, $5000 kPa$, $20000 kPa$ respectively corresponding to $H_2/a=4.0$	32
4.6	Comparison of flexible footing (Ff) and rigid footing (Rf) for variation of I_p with H_1/a from Mohr-Coulomb FE solutions for $\nu_1=\nu_2=0.35$, $E_1=2000kPa$, $E_2=1000kPa$, $H_2/a=4$	33

Chapter 1

Introduction

Many elastic solutions are available to estimate the settlement due to uniform circular load acting on the surface of a two-layer soil system. They include Burmister (1962), Thenn de Barros (1966), Ueshita and Meyerhof (1967), Steinbrenner (1934), Palmer and Barber (1940), Odemark (1949), Vesic (1963), Gerrard (1969), *etc.* In these methods, the top layer is of finite thickness overlies the bottom layer that extends semi-infinately. Elastic solutions are also available to estimate the settlement of uniform circular load acting on a rigid footing resting on a semi-infinite mass [Sneddon (1946)] and on a finite mass [Poulos (1968a)]. However, soil deposition might occur in layers over a rock stratum and the available elastic solutions should be modified when the bottom layer is underlain by a rock stratum or a very stiff soil deposit. Two such instances where the soil profile consisted of two-layer soil deposit, underlain by a rock stratum, are shown in Fig. 1.1. In the present study, charts are proposed to estimate settlements due to uniform circular surface load acting on both flexible and rigid footings resting on such soil profiles - finite two-layer system underlain by a rock stratum (stiff layer).

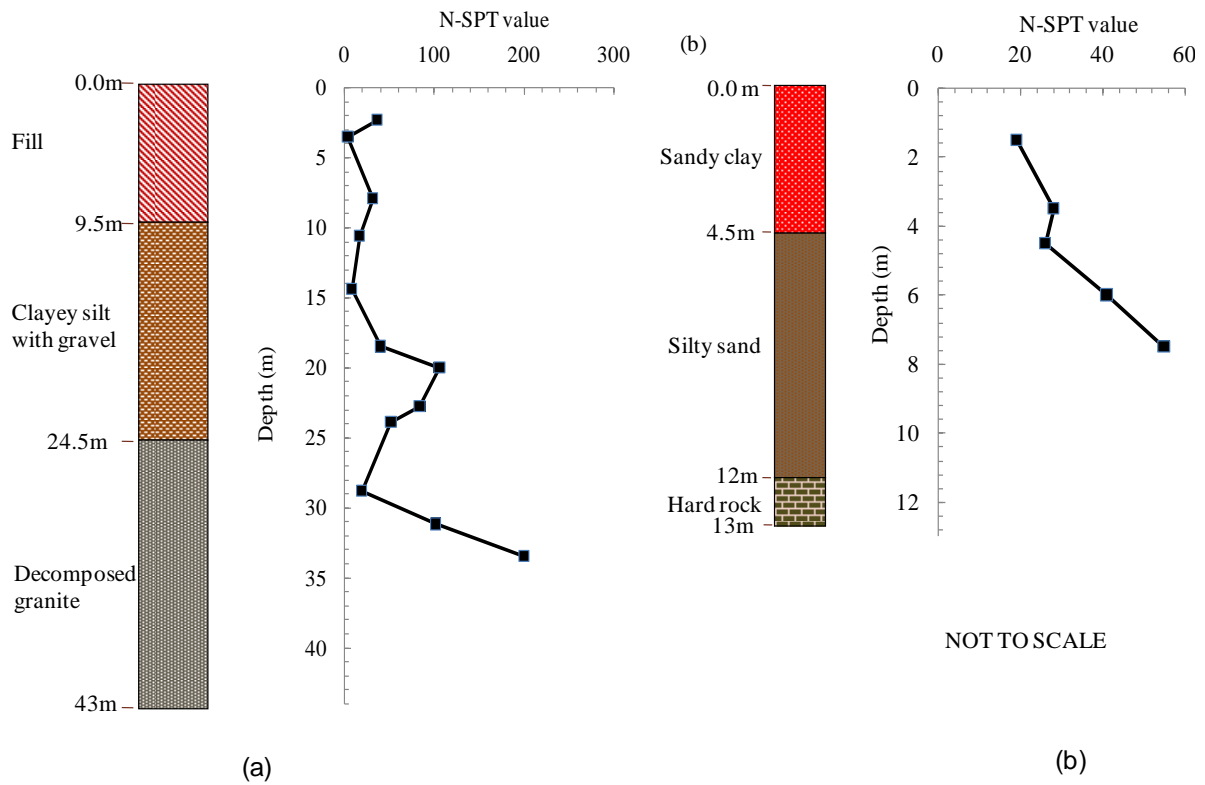


Figure 1.1: Soil profile showing a finite two-layer soil system at (a) Hong Kong [Zhang and Dasaka (2010)] and (b) southern part of Bangalore (Anbazghan and Sitharam [2004])

1.1 Difference in behavior of load acting on flexible and rigid footing

If the footing is subjected to a uniformly distributed load, the contact pressure will be uniform and the settlement of the footing will experience a sagging profile as shown in Fig. 1.2. Boussinesq's equation for vertical deflection on the surface of the elastic half-space with a radius a and a uniform pressure q at $z = 0$ is given by Eq. [1.1]

$$\rho_z = \frac{2(1-\nu^2)qa}{E} \quad [1.1]$$

where, E = Deformation modulus of soil

ν = Poisson's ratio

Perfectly rigid foundation resting on the ground surface subjected to a uniformly distributed load, the footing will undergo a uniform settlement and the contact pressure will be non-uniform (Fig. 1.2). Boussinesq's equation for vertical deflection on the surface of the elastic half-space with a radius a and average contact pressure q at $z = 0$ is given by

$$\rho_z = \frac{\pi(1-\nu^2)qB}{4E} \quad [1.2]$$

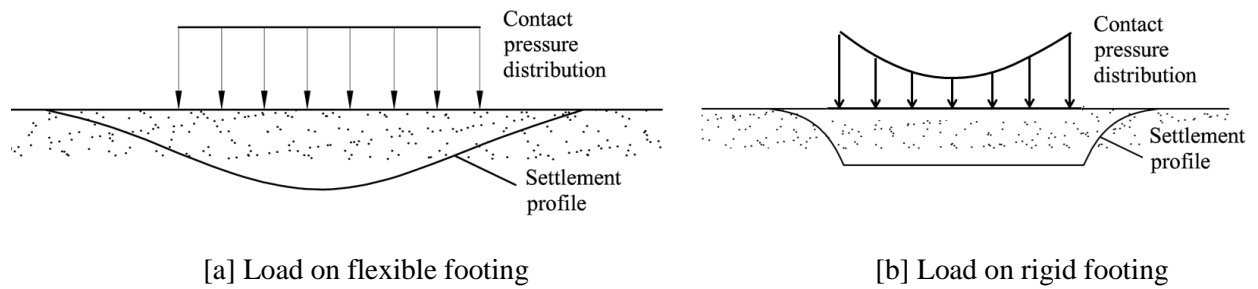


Figure 1.2: Differences in behavior between flexible and rigid footings over clayey soil

In this thesis, the displacement factors to calculate the displacement of the footing, both flexible and rigid, are proposed for various H_1/a , H_2/a , E_1/E_2 , ν_1 , and ν_2 values, where H_1 is the top layer thickness, H_2 is the bottom layer thickness, a is the radius of the circular loading, E_1 and E_2 are the deformation moduli of top and bottom layers, and ν_1 and ν_2 are the Poisson's ratio of top and bottom layers, respectively. Linear stress-strain and linear elastic- perfectly plastic (Mohr-Coulomb) constitutive models were used for the soil deposits. In the analysis using Mohr-Coulomb model, displacement factors are proposed at various levels of settlement ratios of the footing. Modeling was performed using the commercially available finite element analysis software - PLAXIS 2D.

1.2 Problem statement

A uniform circular load on flexible footing and rigid footing of intensity q acts on an area with radius a and a rigid boundary underlies two-layer soil system is shown in Fig. 1.3. The thickness of the top soil layer is H_1 with deformation modulus E_1 and Poisson's ratio ν_1 , and the bottom layer is of thickness H_2 with elasticity properties E_2 and Poisson's ratio ν_2 . Settlement factors are to be proposed to estimate the settlements at the center of circular load for cases where [1] a soft soil layer overlies a stiff layer ($E_1/E_2 < 1.0$), and [2] a stiff soil layer overlies a soft layer ($E_1/E_2 > 1.0$) for finite two-layered soil profiles.

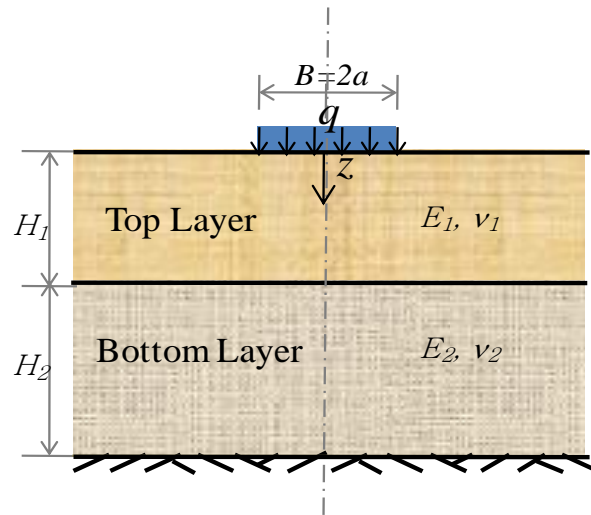


Figure 1.3: Definition sketch

1.3 Organization of the study

Chapter 2 discusses the existing literature of elastic solutions for the calculation of settlements for semi-infinite homogenous elastic soil, finite soil layer underlain by a stiff layer, and multiple layer of soil profiles.

Chapter 3 deals with the estimation of settlements for finite two-layer system using linear stress-strain behavior and it is compared with finite element solutions for loading on both rigid and flexible footings.

Chapter 4 deals with the estimation of settlements for finite two-layer system using non-linear behavior of soil deposits based on finite element solutions for loading on both rigid and flexible footings.

Summary and conclusions based on present study are given in Chapter 5.

Chapter 2

Literature review

2.1 Elastic solutions for Homogenous finite layer

Poulos [1968a] provided the plot of displacement influence factor versus thickness ratios for Poisson's ratio values of 0, 0.2, 0.4 and 0.5 for the circular load acting on the rigid footing resting on homogenous finite layer as shown in Fig. 2.1. Vertical displacement can be calculated by using Eq. [2.1].

$$\rho_z = \pi(1-\nu^2) \frac{P_{av} a I_\rho}{E} \quad [2.1]$$

where, p_{av} = Average applied pressure

a = Radius of circular load

E = Deformation modulus of soil

ν = Poisson's ratio

h = Depth of the homogenous finite layer

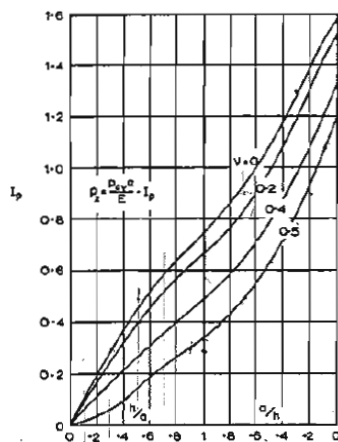


Figure 2.1: Influence factors for the vertical displacement of rigid circle (Poulos [1968a])

2.2 Elastic solutions for Homogenous semi-infinite soil

Boussinesq proposed equations to calculate the stresses, strains and deflections beneath the center of a circular load when the load is applied on the homogenous semi-infinite soil.

Foster and Ahlvin [1954] presented the plots to calculate vertical stresses, radial stresses, tangential stresses, shear stresses and vertical deflections at various points within an elastic half space under circular load acting on flexible footing. The plot of deflection factor, I_ρ , versus depth in radii, z/a , for circular load acting on flexible footing for the Poisson's ratio equal to 0.5 is shown in Fig. 2.2. Vertical deflections, ρ_z , can be calculated by using Eq. [2.2].

$$\rho_z = \frac{qB}{E} I_\rho \quad [2.2]$$

Where, B =Diameter of the circular area

q =Uniformly distributed load

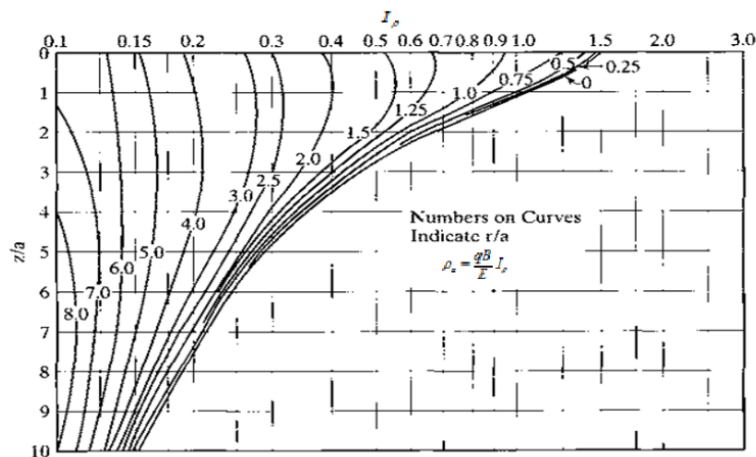


Figure 2.2: Vertical deflection due to circular loading for Poisson's ratio equal to 0.5 (Foster and Ahlvin [1954])

Ahlvin and Ulery [1962] presented a series of equations and tables to estimate the stresses, strains and deflections due to circular load on flexible footing for a given Poisson's ratio.

Sneddon [1946] proposed an equation for vertical surface displacement of rigid circular load acting on semi-infinite mass is shown in Eq. [2.3].

$$\rho_z = \frac{p_{av} a I_\rho}{E} \quad [2.3]$$

2.3 Elastic solutions for two-layered soil system (top layer is finite and bottom layer is semi-infinite)

Burmister [1962] provided the plots of displacement factors versus H_1/a (ratio of top layer thickness to the radius of circular load) to calculate the deflection at the center of the circular load acting on flexible footing for Poisson's ratios equal to 0.2, 0.4 and 0.5. Plots of displacement factors versus H_1/a for Poisson's ratio equal to 0.5 is shown in Fig. 2.3. Vertical deflections, ρ_z , can be calculated by using Eq. [2.4].

$$\rho_z = \frac{1.5qaI_\rho}{E_2} \quad [2.4]$$

where, E_2 = Deformation modulus of bottom layer

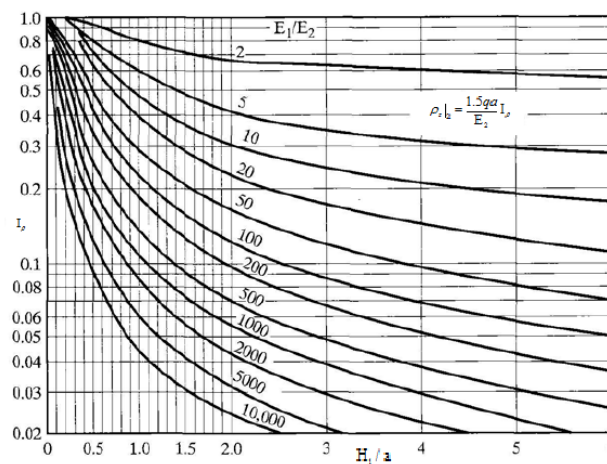


Figure 2.3: Vertical surface deflections for two-layered systems for $\nu_1=\nu_2= 0.5$ (After Burmister [1943])

Ueshita and Meyerhof [1967] provided an equivalent value of deformation modulus (E_e) which may be used as a displacement influence factor for the center of the circular load acting on the flexible footing on two-layer system. The variation of E_e/E_2 with H_1/a and E_1/E_2 (ratio of deformation modulus of top and bottom layers) for Poisson's ratio equal to 0.5 is shown in Fig. [2.4]. Vertical displacements, ρ_z , can be calculated by using Eq. [2.5].

$$\rho_z = \frac{1.5qa}{E_e} \quad [2.5]$$

where, E_1/E_2 = Ratio of deformation modulus of top and bottom layers

E_e = Equivalent deformation modulus

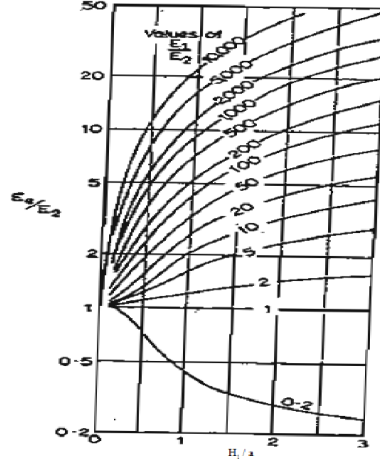


Figure 2.4: Equivalent modulus E_e of two-layered systems for $\nu_1=\nu_2=0.5$ (Ueshita and Meyerhof [1967])

2.4 Elastic solution for Multi-layer soil system

Steinbrenner [1934] proposed a method to estimate the vertical surface displacement of a loaded area on assumption that the stress distribution within the layered system is identical with the Boussinesq's stress distribution for a homogenous semi-infinite mass. It was originally applied to the problem of a single layer underlain by the rough rigid base, and for the case of rectangular load acting on the flexible footing. It can be extended to any number of layers. Steinbrenner's approximation is most satisfactory for layered system in which the modulus increases rather than it decreases with depth.

The settlement, $\rho_z|_n$, for the multilayer system is given by Eq. [2.6].

$$\rho_z|_n = qB \left[\sum_{i=1}^n \frac{(1-\nu_i^2)}{E_i} (I_{\rho_i} - I_{\rho_{i-1}}) \right] \quad [2.6]$$

Where, B = Shorter side of rectangle

Palmer and Barber [1940] assumes that upper layer of the thickness H_1 , modulus E_1 and $\nu=\nu_1$ is replaced by an equivalent thickness (h_e) of lower layer material (E_2 and $\nu=\nu_2$). Equivalent thickness, h_e , can be obtained from Eq. [2.7]. Vertical displacement is then obtained by adding the vertical displacement, ρ_1 , at a depth h_e and the displacement within the upper layer, ρ_2 , as given in Eq. [2.8]. Palmer and Barber's method can be extended to multi-layer system by repeated replacement of overlying layers by an equivalent thickness of the lower most material.

$$h_e = h_1 \left(\frac{E_1(1-\nu_2)^2}{E_2(1-\nu_1)^2} \right)^{1/3} \quad [2.7]$$

$$\rho_z = \rho_1 + \rho_2 \quad [2.8]$$

Vesic [1963] prepared charts for both uniform circular load and for circular load acting on a rigid circular footing. These charts are shown in Fig. 2.5. They are based on the Boussinesq's stress distribution (like Steinbrenner's method) for a uniform semi-infinite mass. Vesic's approximation is most satisfactory for layered system in which the modulus increases rather than it decreases with the depth. The vertical displacements can be calculated from the displacement factors corresponding to depth in radii from Eq. [2.6].

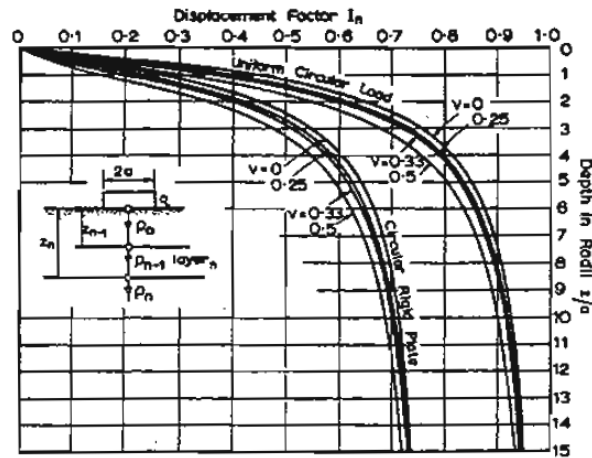


Figure 2.5: Approximate displacement factors for layered systems for $v_1=v_2=0.5$ (Vesic [1963])

Chapter 3

Settlement of Finite Two-layer System using Linear Stress-Strain Behavior

For loads within the elastic range, settlements can be estimated using linear stress-strain model. In this chapter, settlement of footing (both flexible and rigid) resting on finite two-layer system is estimated using linear stress-strain response of the soil. The bottom layer is resting on a rock stratum or a very stiff layer.

3.1 Load on Flexible Footing

3.1.1 Elastic Solution

Steinbrenner (1934) proposed a method to estimate the surface settlement at the center of a circular loaded area for a multi-layer system. For a multi-layered system of n layers, equation for the settlement at the center is given by

$$\rho_z|_n = qB \left[\sum_{i=1}^n \frac{(1-\nu_i^2)}{E_i} (I_{\rho i} - I_{\rho i-1}) \right] \quad [3.1]$$

Where, E_i and ν_i are the elastic parameters of layer i ,

B is the diameter of loading area = $2a$,

$I_{\rho i}$ is the vertical displacement factor corresponding to a depth factor h_i/B , h_i is the depth below the ground surface of the top of layer i

For a two-layer system, Eq. 3.1 becomes

$$\rho_z|_2 = qB \left[\frac{(1-\nu_1^2)}{E_1} (I_{\rho 1} - I_{\rho 0}) + \frac{(1-\nu_2^2)}{E_2} (I_{\rho 2} - I_{\rho 1}) \right] \quad [3.2]$$

where, $I_{\rho 0}$, $I_{\rho 1}$ and $I_{\rho 2}$ represent the vertical displacement factors corresponding to depths $z = 0$, $z = H_1$ and $z = (H_1 + H_2)$. Vesic's chart, shown in Fig. 3.1, can be used to obtain the vertical displacement influence factors.

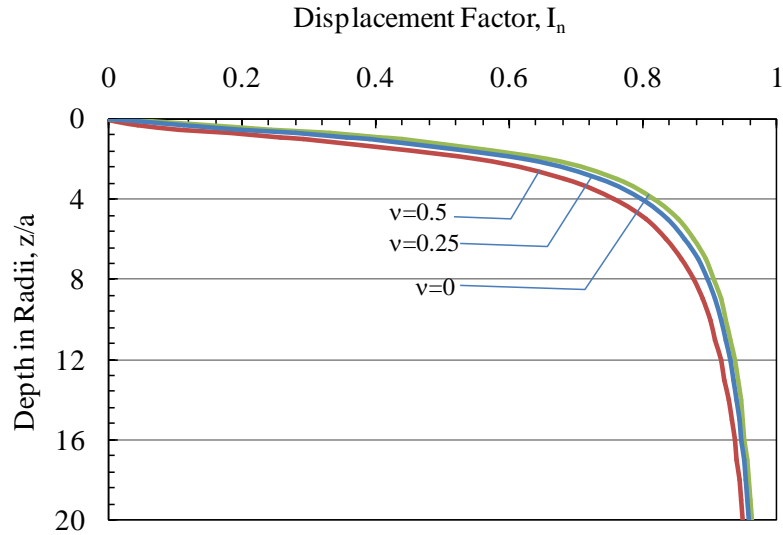


Figure 3.1: Displacement factors for layered systems for load on flexible footing (modified after Vesic [1963])

The first term of Eq. 3.2 represents the settlement of top layer of finite thickness H_1 and the second term corresponds to the settlement of bottom layer of finite thickness H_2 assuming a homogenous soil deposit with moduli of elasticity E_1 and E_2 for the top and bottom layers, respectively. Steinbrenner's method is based on the assumption that the stress distribution within the layered system is identical with that of the stress distribution for a homogenous semi-infinite layer. Hence, the applicability of Steinbrenner's method for layered system will depend on the vertical stress distribution for the two-layered system in comparison to that for a homogenous semi-infinite layer. The vertical distribution was obtained for a finite two-layer soil system and for a homogenous semi-infinite layer for two cases- (a) soft layer overlying stiff layer ($E_1/E_2 < 1.0$), and (b) stiff layer overlying soft layer ($E_1/E_2 > 1.0$). The stress distribution was obtained using commercially available Finite Element software PLAXIS 2D Version 8.2 for an applied stress at the surface $q = 500$ kPa and radius of circular loaded area $a = 1.0$ m.

Fig. 3.2 shows the vertical stress contours for a uniform elastic medium of constant E and for a two-layer system with $E_1/E_2 = 0.1$. It can be seen from the figure that the vertical stress distribution for the two-layer system is identical to that for a uniform elastic medium. Eq. 3.2 can, hence, give a reasonably good estimate of the settlement of the two-layer system with $E_1/E_2 < 1.0$ using Steinbrenner's approach.

Fig. 3.3 shows the vertical stress contours for a uniform elastic medium of constant E and for a two-layer system with $E_1/E_2 = 10$. The difference in the vertical stress distribution is significant for the two cases, the bottom layer experiences a vertical stress of only about $0.3q$ at the top of the bottom layer

(at $z = H_1$) in a two-layer system, whereas a much higher value of $0.7q$ is transferred at the same level for a uniform elastic medium. Due to significant difference in the stress distribution, the settlement of a two-layer system with $E_1/E_2 > 1.0$ cannot be predicted correctly using Steinbrenner's method (Eq. 3.2).

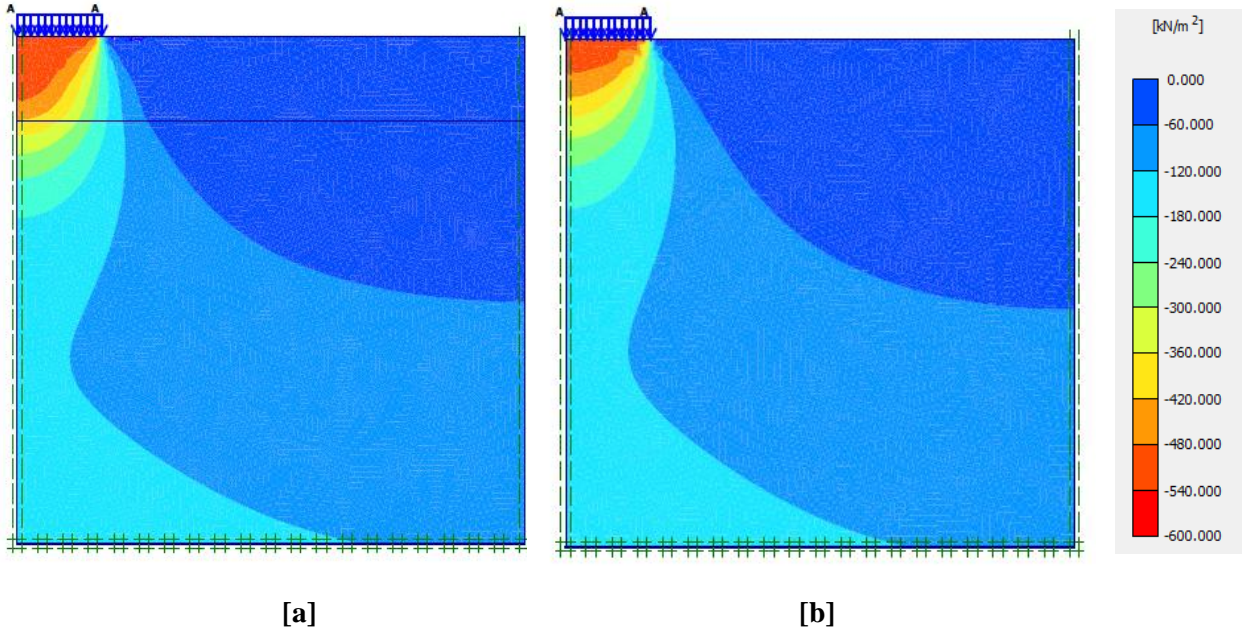


Figure 3.2: Comparison of vertical stress contours for $q=500$ kPa and $a=1\text{m}$ for [a] uniform elastic medium (constant E), $\nu=0.5$, and [b] two-layer system with $H_1=1\text{m}$, $E_1=1\text{MPa}$, $\nu_1=0.5$; $H_2=5\text{m}$, $E_2=10\text{MPa}$, $\nu_2=0.5$

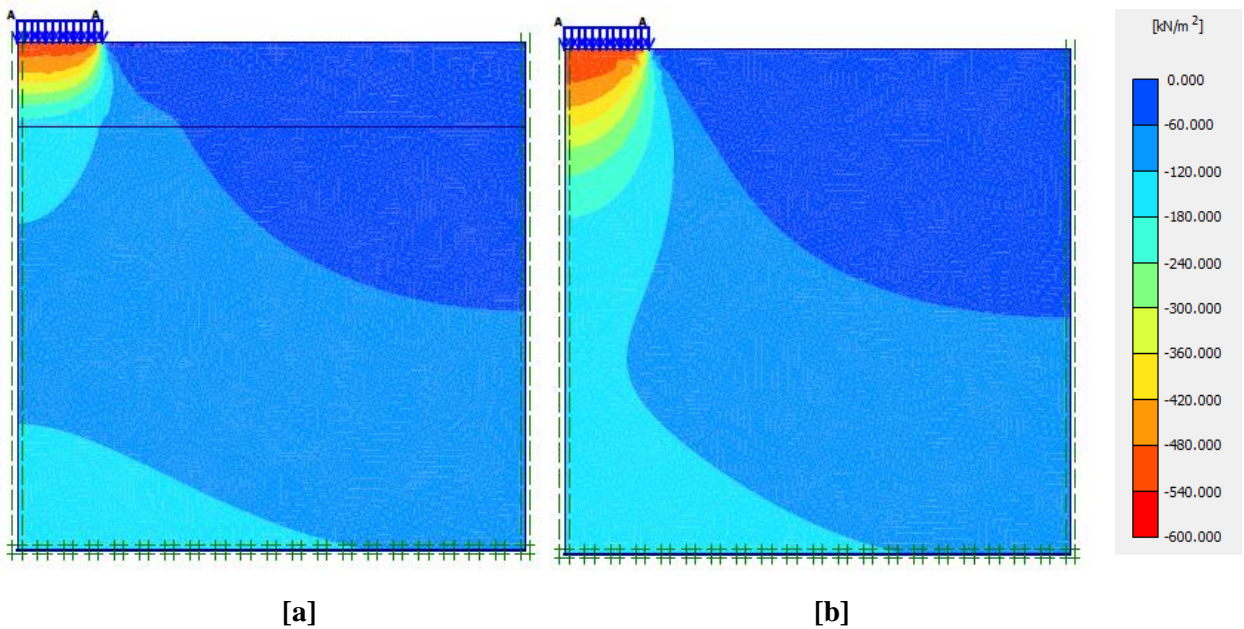


Figure 3.3: Comparison of vertical stress contours for $q= 500$ kPa and $a=1\text{m}$ for [a] uniform elastic medium (constant E), $\nu=0.5$, and [b] two-layer system with $H_1=1\text{m}$, $E_1=10\text{MPa}$, $\nu_1=0.5$; $H_2=5\text{m}$, $E_2=1\text{MPa}$, $\nu_2=0.5$

3.1.2 Finite Element Analysis

The software PLAXIS 2D Version 8.2 was used to obtain settlements using Finite Element (FE) method. Due to axi-symmetry, only one-half of the model was considered. Convergence of settlement at the center of the loaded area was checked by varying the size of the mesh and the distance of lateral boundary from the axis of symmetry. Based on preliminary studies, the right boundary was fixed at a distance of $25a$ from the axis of symmetry, this distance is found to model the semi-infinite lateral extent of the deposit. Mesh coarseness was set to ‘very fine’ to discretize the domain. For example, Fig. 3.4 shows the FE model for the case with radius $a=1.0\text{m}$, $H_1/a=2.0$ and $H_2/a=4.0$. This geometry is divided into 1036 elements with an average element size of about 380mm. 15-noded triangular elements were chosen and the boundary conditions include restraining the displacements of nodes in r - direction ($u_r=0$) along the axis of symmetry and the right boundary, and restraining the displacements of nodes in both r - and z - directions ($u_r=0$ and $u_z=0$) along the bottom rigid boundary.

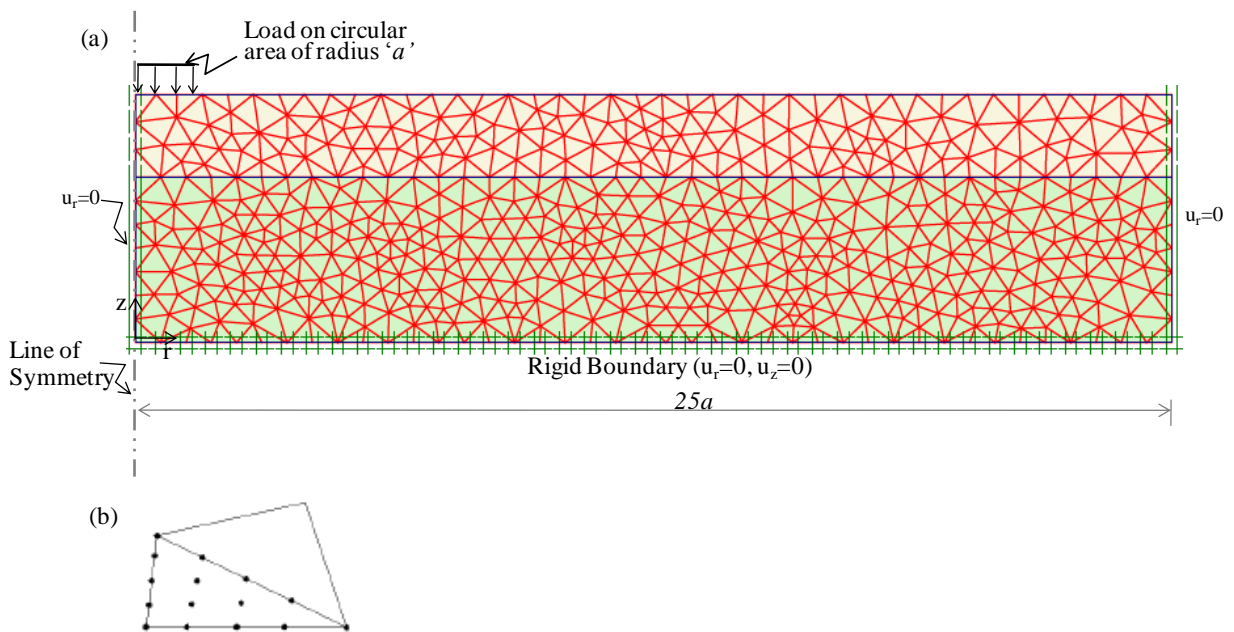


Figure 3.4: Finite element modeling: (a) meshing, and (b) 15-noded triangular element used for discretization

3.1.3 Results

The vertical displacement factor I_ρ for the two-layer system is proposed for various values of $H_1 = 0.1$ -to- 6.0m , $H_2 = 1.0$ -to- 6.0m , $E_1/E_2 = 0.01$ -to- 100 and $\nu_1 = \nu_2 = 0.2$ -to- 0.5 . This factor I_ρ is obtained by equating the settlement of two-layer system $\rho_z|_2$ to qBI_ρ/E_2

$$i.e., \rho_z|_2 = \frac{qB}{E_2} I_\rho$$

$$\Rightarrow I_\rho = \frac{\rho_z | E_2}{qB} \quad [3.3]$$

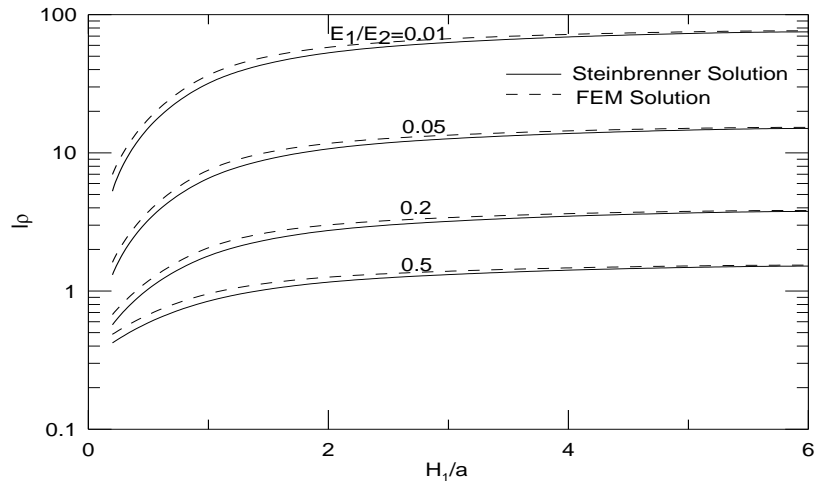
For the two-layer system with $E_1/E_2 < 1.0$, both elastic and finite element solutions are presented, whereas for the case $E_1/E_2 > 1.0$, only finite element solution is given as the elastic solution based on Steinbrenner's method is not applicable.

3.1.3.1 Displacement Factors for the Case $E_1/E_2 < 1.0$

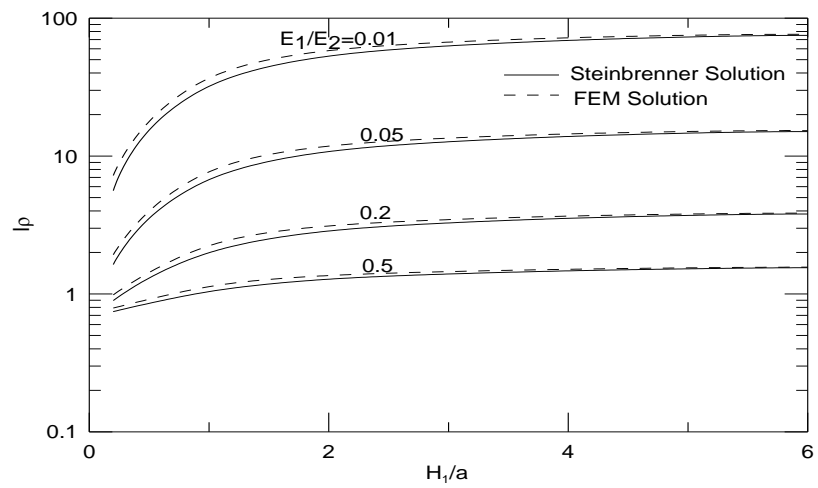
Table 3.1 shows I_ρ values of H_1/a from 0.2-6.0 corresponding to H_2/a values 1, 2, 4 and 6 respectively, for $E_1/E_2=0.01$ -to-1.0 and $\nu_1=\nu_2=0.2, 0.35, 0.5$ based on finite element solution. Figures 3.5 and 3.6 show the variations of I_ρ with H_1/a and H_2/a , respectively, for $E_1/E_2=0.01$ -to-0.5 and $\nu_1=\nu_2=0.5$ based on Steinbrenner's and finite element methods.

Figure 3.5 shows that elastic and FE solutions show good agreement, except for $H_1/a < 0.6$ and $E_1/E_2=0.01$ with FE solution giving a higher I_ρ compared to elastic solution. I_ρ increases nonlinearly with increase in the thickness of the top, softer layer. The rate of increase of I_ρ with H_1/a is higher for low H_1/a (up to $H_1/a=1.0$) compared to that at large H_1/a . This rate of increase is higher at low E_1/E_2 (for *e.g.*, $E_1/E_2 = 0.01, 0.05$) than at relatively high E_1/E_2 (for *e.g.*, $E_1/E_2 = 0.2, 0.5$). For instance, I_ρ value increases from 22.2 to 41.5 as H_1/a increases from 1.0 to 2.0, whereas thereafter I_ρ only increases from 0.6 to 0.9 for the same H_1/a for $E_1/E_2 = 0.01$ and $E_1/E_2 = 0.5$, respectively.

Figure 3.6 show the variation of I_ρ with H_2/a for $H_1/a= 0.5$ and 2.0. Figure 3.6 shows that the effect of H_2/a on settlement is not significant for a relatively thick top deposit ($H_1/a=2.0$), whereas for the case of $H_1/a=0.5$, the thickness of bottom layer affect the I_ρ values for $E_1/E_2 = 0.2$ and 0.5. For a low thickness of soft top layer over stiff bottom layer ($H_1/a=0.5$), displacement factor from FE solution is 18-20 % and 10-16% higher than that of elastic solution for $E_1/E_2= 0.01$ and 0.05, respectively. However, for $E_1/E_2=0.2$ or 0.5, both elastic and FE solutions give similar results. For the case of thick soft layer over stiff bottom layer ($H_1/a=2.0$), I_ρ values obtained from elastic and FE solutions show good agreement.

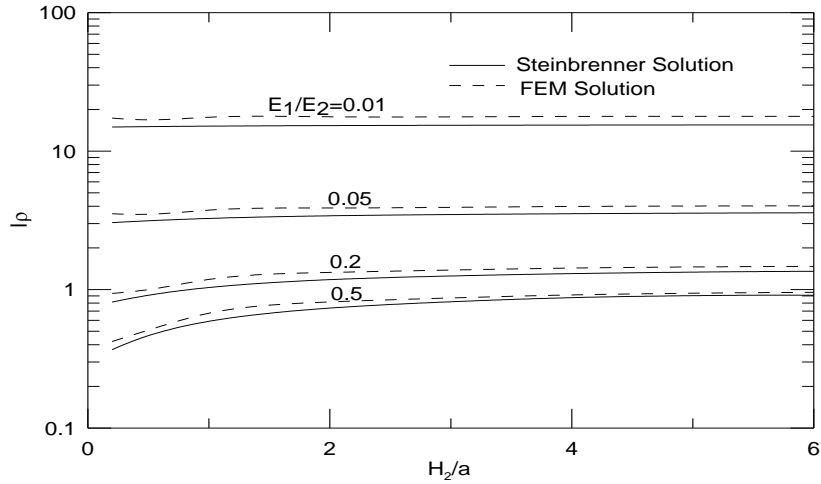


(a)

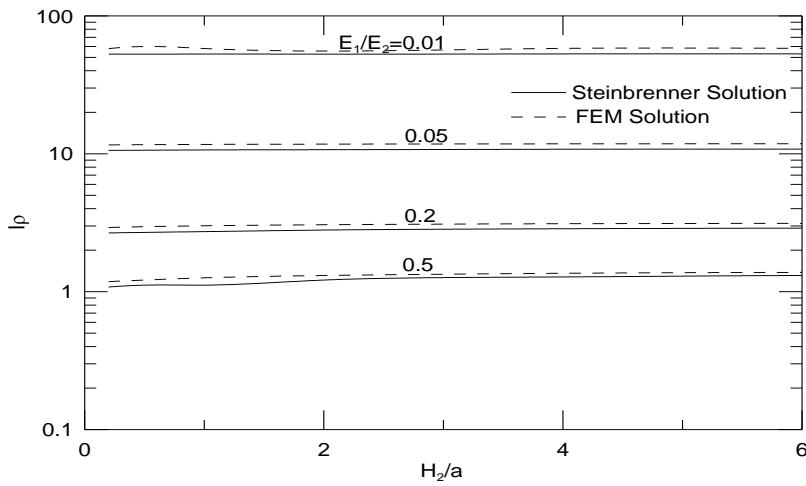


(b)

Figure 3.5: Variation of I_ρ with H_1/a from elastic and finite element solutions for $\nu_1=\nu_2=0.35$, $E_1/E_2=0.01-1.0$ and corresponding to (a) $H_2/a=1.0$ and (b) $H_2/a=4.0$



(a)



(b)

Figure 3.6: Variation of I_ρ with H_1/a from elastic and finite element solutions for $\nu_1=\nu_2=0.35$, $E_1/E_2=0.01-1.0$ and corresponding to (a) $H_1/a=0.5$ and (b) $H_1/a=2.0$

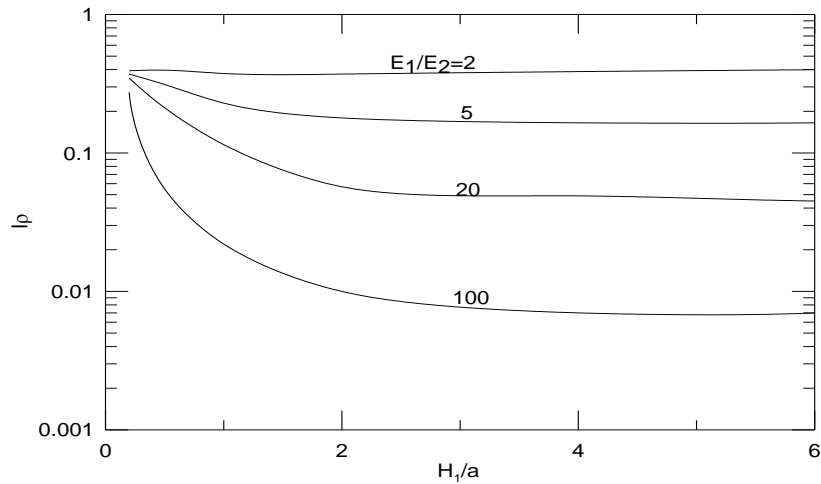
3.1.3.2 Displacement Factors for the Case $E_1/E_2 > 1.0$

Table 3.2 shows I_ρ values of H_1/a ranging from 0.2-to-6.0 corresponding to H_2/a values 1, 2, 4, and 6 respectively, for $E_1/E_2=2$ -to-100 and $\nu_1=\nu_2=0.2, 0.35, 0.5$ based on finite element solution. Figures 3.7 and 3.8 show the variations of I_ρ with H_1/a and H_2/a , respectively, for $E_1/E_2=2$ -to-100 and $\nu_1=\nu_2=0.5$ based on finite element solution.

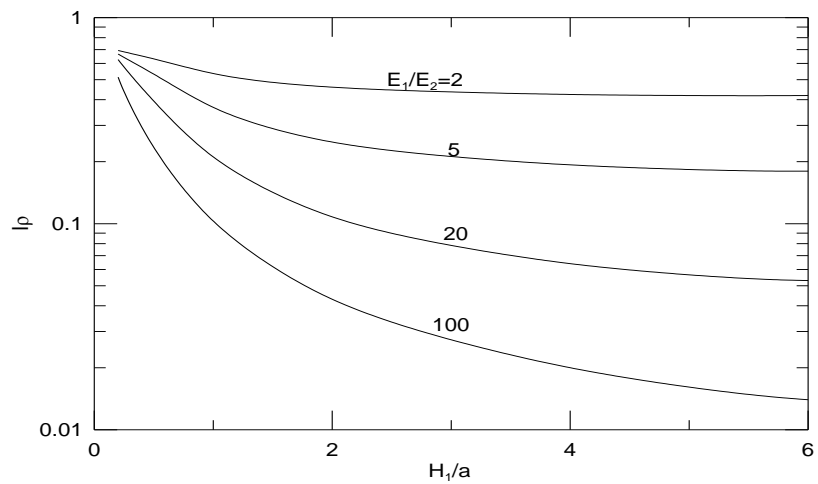
Figure 3.7 show that as the thickness of the top stiff layer increases, the settlement of the two-layer system decreases. The rate of decrease of I_ρ with H_1/a is higher for relatively low H_1/a (till $H_1/a = 3.0$) than for higher H_1/a values. This decrease increases with increase in E_1/E_2 values. For instance, I_ρ

decreases by 81% as H_1/a increases from 0.5-to-2.0 for $E_1/E_2=100$, whereas it is only decreases by 4% for the same increase in H_1/a (0.5-to-2.0m) for $E_1/E_2=5$.

For a given thickness of top stiff layer, I_ρ values increase with increase in thickness of bottom soft layer, as shown in Fig. 3.8. The rate of increase of I_ρ with H_2/a is higher for larger E_1/E_2 ratios compared to that of lower E_1/E_2 ratios. For H_2/a varying from 1.0-to-6.0, I_ρ increases by 137% and by 40% for $E_1/E_2=100$ and $E_1/E_2=2$, respectively, for $H_1/a=2.0$.

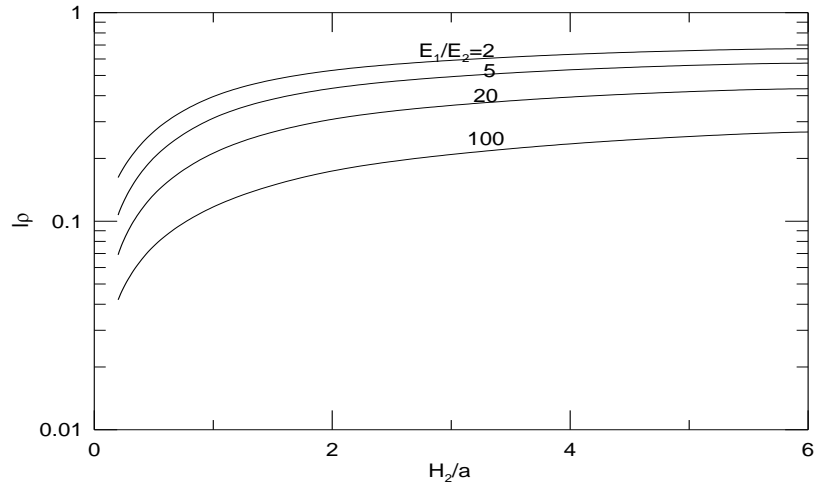


(a)

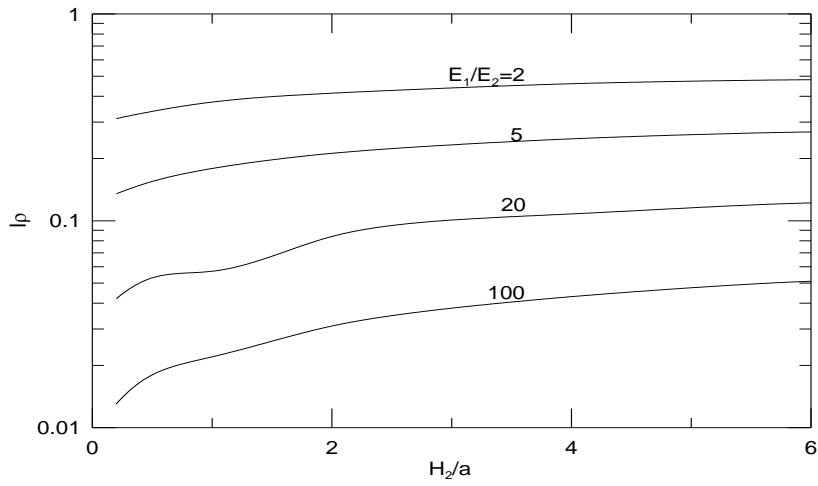


(b)

Figure 3.7: Variation of I_ρ with H_1/a from elastic and finite element solutions for $\nu_1=\nu_2=0.5$, $E_1/E_2=2-100$ and corresponding to (a) $H_2/a=1.0$ and (b) $H_2/a=4.0$



(a)



(b)

Figure 3.8: Variation of I_ρ with H_1/a from elastic and finite element solutions for $\nu_1=\nu_2=0.5$, $E_1/E_2=2-100$ and corresponding to (a) $H_1/a=0.5$ and (b) $H_1/a=2.0$

Table 3.1: I_ρ values for $E_1/E_2 > 1.0$ using finite element solution

$E_1/E_2=0.$	H_1/a	$\nu=0.2$	$\nu=0.35$	$\nu=0.5$
$H_2/a=1$	0.2	8.021	5.282	1.712
	0.5	20.40	15.154	8.173
	1.0	38.88	31.844	22.162
	2.0	60.77	52.886	41.557
	4.0	77.05	68.922	56.845
	6.0	83.17	74.995	62.687
$H_2/a=2$	0.2	8.209	5.464	1.881
	0.5	20.55	15.300	8.310
	1.0	38.98	31.947	22.260
	2.0	60.83	52.944	41.612
	4.0	77.07	68.947	56.868
	6.0	83.18	75.009	62.700
$H_2/a=4$	0.2	8.353	5.608	2.081
	0.5	20.67	15.421	8.426
	1.0	39.08	32.041	22.350
	2.0	60.89	53.005	41.671
	4.0	77.10	68.978	56.899
	6.0	83.20	75.028	62.719
$H_2/a=6$	0.2	8.411	5.664	2.072
	0.5	20.72	15.472	8.475
	1.0	39.12	32.084	22.391
	2.0	60.92	53.036	41.701
	4.0	77.12	68.997	56.917
	6.0	83.22	75.040	62.731

$E_1/E_2=0.05$	H_1/a	$\nu=0.2$	$\nu=0.35$	$\nu=0.5$
$H_2/a=1$	0.2	1.899	1.314	0.547
	0.5	4.334	3.265	1.838
	1.0	7.952	6.538	4.588
	2.0	12.239	10.660	8.390
	4.0	15.440	13.813	11.397
	6.0	16.649	15.013	12.551
$H_2/a=2$	0.2	2.088	1.497	0.716
	0.5	4.484	3.411	1.976
	1.0	8.058	6.641	4.687
	2.0	12.297	10.718	8.445
	4.0	15.465	13.838	11.421
	6.0	16.663	15.027	12.564
$H_2/a=4$	0.2	2.232	1.640	0.853
	0.5	4.607	3.532	2.092
	1.0	8.152	6.735	4.777
	2.0	12.359	10.778	8.504
	4.0	15.496	13.870	11.451
	6.0	16.682	15.046	12.583
$H_2/a=6$	0.2	2.289	1.696	0.907
	0.5	4.657	3.583	2.140
	1.0	8.195	6.778	4.818
	2.0	12.390	10.810	8.534
	4.0	15.515	13.889	11.469
	6.0	16.695	15.059	12.595

$E_1/E_2=0.2$	H_1/a	$\nu=0.2$	$\nu=0.35$	$\nu=0.5$
$H_2/a=1$	0.2	0.752	0.570	0.328
	0.5	1.322	1.036	0.651
	1.0	2.153	1.793	1.293
	2.0	3.139	2.742	2.171
	4.0	3.887	3.481	2.875
	6.0	4.176	3.767	3.151
$H_2/a=2$	0.2	0.940	0.753	0.498
	0.5	1.471	1.182	0.788
	1.0	2.258	1.896	1.392
	2.0	3.197	2.800	2.226
	4.0	3.912	3.505	2.899
	6.0	4.189	3.780	3.164
$H_2/a=4$	0.2	1.085	0.896	0.635
	0.5	1.594	1.303	0.904
	1.0	2.353	1.990	1.482
	2.0	3.258	2.861	2.285
	4.0	3.944	3.537	2.929
	6.0	4.209	3.799	3.182
$H_2/a=6$	0.2	1.142	0.952	0.689
	0.5	1.645	1.354	0.953
	1.0	2.396	2.033	1.523
	2.0	3.290	2.892	2.315
	4.0	3.963	3.556	2.948
	6.0	4.221	3.812	3.195

$E_1/E_2=0.5$	H_1/a	$\nu=0.2$	$\nu=0.35$	$\nu=0.5$
$H_2/a=1$	0.2	0.522	0.422	0.284
	0.5	0.719	0.590	0.413
	1.0	0.993	0.844	0.634
	2.0	1.319	1.159	0.927
	4.0	1.577	1.414	1.171
	6.0	1.681	1.517	1.271
$H_2/a=2$	0.2	2.088	1.497	0.716
	0.5	4.484	3.411	1.976
	1.0	8.058	6.641	4.687
	2.0	12.297	10.718	8.445
	4.0	15.465	13.838	11.421
	6.0	16.663	15.027	12.564
$H_2/a=4$	0.2	2.232	1.640	0.853
	0.5	4.607	3.532	2.092
	1.0	8.152	6.735	4.777
	2.0	12.359	10.778	8.504
	4.0	15.496	13.870	11.451
	6.0	16.682	15.046	12.583
$H_2/a=6$	0.2	0.912	0.803	0.645
	0.5	1.042	0.908	0.715
	1.0	1.236	1.084	0.864
	2.0	1.470	1.309	1.072
	4.0	1.653	1.489	1.243
	6.0	1.727	1.563	1.314

Table 3.2: I_ρ values for $E_1/E_2 > 1.0$ using finite element solution

$E_1/E_2=2$	H_1/a	$\nu=0.2$	$\nu=0.35$	$\nu=0.5$
$H_2/a=1$	0.2	0.456	0.392	0.267
	0.5	0.451	0.397	0.290
	1.0	0.425	0.376	0.282
	2.0	0.417	0.371	0.288
	4.0	0.430	0.384	0.303
	6.0	0.442	0.393	0.307
$H_2/a=2$	0.2	0.630	0.570	0.453
	0.5	0.580	0.530	0.430
	1.0	0.510	0.460	0.369
	2.0	0.459	0.412	0.350
	4.0	0.447	0.398	0.311
	6.0	0.455	0.402	0.308
$H_2/a=4$	0.2	0.750	0.690	0.575
	0.5	0.675	0.625	0.535
	1.0	0.575	0.530	0.441
	2.0	0.500	0.450	0.356
	4.0	0.474	0.418	0.315
	6.0	0.480	0.420	0.308
$H_2/a=6$	0.2	0.790	0.730	0.605
	0.5	0.710	0.660	0.560
	1.0	0.610	0.560	0.456
	2.0	0.530	0.471	0.361
	4.0	0.500	0.436	0.315
	6.0	0.489	0.429	0.319

$E_1/E_2=5$	H_1/a	$\nu=0.2$	$\nu=0.35$	$\nu=0.5$
$H_2/a=1$	0.2	0.423	0.372	0.244
	0.5	0.350	0.313	0.216
	1.0	0.259	0.229	0.158
	2.0	0.202	0.179	0.129
	4.0	0.184	0.163	0.124
	6.0	0.185	0.163	0.123
$H_2/a=2$	0.2	0.585	0.545	0.438
	0.5	0.464	0.435	0.352
	1.0	0.327	0.299	0.232
	2.0	0.233	0.209	0.184
	4.0	0.198	0.174	0.128
	6.0	0.198	0.167	0.124
$H_2/a=4$	0.2	0.695	0.665	0.570
	0.5	0.550	0.530	0.464
	1.0	0.387	0.362	0.304
	2.0	0.268	0.238	0.179
	4.0	0.224	0.192	0.129
	6.0	0.223	0.189	0.124
$H_2/a=6$	0.2	0.735	0.700	0.600
	0.5	0.585	0.560	0.489
	1.0	0.417	0.387	0.319
	2.0	0.294	0.257	0.182
	4.0	0.249	0.209	0.130
	6.0	0.230	0.196	0.129

$E_1/E_2=20$	H_1/a	$\nu=0.2$	$\nu=0.35$	$\nu=0.5$
$H_2/a=1$	0.2	0.390	0.347	0.210
	0.5	0.242	0.213	0.124
	1.0	0.134	0.115	0.064
	2.0	0.075	0.057	0.039
	4.0	0.057	0.049	0.032
	6.0	0.056	0.048	0.031
$H_2/a=2$	0.2	0.535	0.510	0.399
	0.5	0.331	0.308	0.226
	1.0	0.178	0.160	0.110
	2.0	0.093	0.080	0.072
	4.0	0.069	0.058	0.033
	6.0	0.069	0.056	0.031
$H_2/a=4$	0.2	0.635	0.063	0.540
	0.5	0.404	0.391	0.327
	1.0	0.222	0.203	0.156
	2.0	0.120	0.099	0.057
	4.0	0.095	0.075	0.033
	6.0	0.094	0.074	0.032
$H_2/a=6$	0.2	0.068	0.660	0.600
	0.5	0.438	0.420	0.351
	1.0	0.249	0.224	0.164
	2.0	0.145	0.117	0.058
	4.0	0.119	0.092	0.033
	6.0	0.099	0.077	0.032

$E_1/E_2=10$	H_1/a	$\nu=0.2$	$\nu=0.35$	$\nu=0.5$
$H_2/a=1$	0.2	0.316	0.274	0.149
	0.5	0.139	0.118	0.055
	1.0	0.062	0.052	0.022
	2.0	0.028	0.022	0.010
	4.0	0.021	0.017	0.007
	6.0	0.021	0.016	0.006
$H_2/a=2$	0.2	0.437	0.407	0.296
	0.5	0.195	0.174	0.109
	1.0	0.081	0.069	0.041
	2.0	0.040	0.031	0.030
	4.0	0.034	0.025	0.007
	6.0	0.033	0.025	0.006
$H_2/a=4$	0.2	0.530	0.510	0.424
	0.5	0.249	0.229	0.172
	1.0	0.110	0.092	0.052
	2.0	0.066	0.049	0.013
	4.0	0.059	0.042	0.007
	6.0	0.058	0.042	0.007
$H_2/a=6$	0.2	0.565	0.545	0.456
	0.5	0.279	0.254	0.186
	1.0	0.136	0.109	0.053
	2.0	0.091	0.066	0.013
	4.0	0.084	0.060	0.007
	6.0	0.064	0.046	0.007

3.1.4. Case Study and Validation

1. Ueshita and Meyerhof (1967) proposed a plot to estimate settlements at the center of a circular area for the case of finite top layer overlying a semi-infinite bottom layer. To compare these results with the present study, the thickness of bottom layer and distance of lateral boundary from the axis of symmetry were taken as $40a$ in the Finite Element model. Table 3.3 provides the comparison of I_p values from the present study and Ueshita and Meyerhof (1967) for $H_1/a = 0.5$ -to- 3.0 for $E_1/E_2 = 0.2, 2, 5, 20$ and 100 . In most cases, the proposed settlement factors presented in the study are within 10% of the values proposed by Ueshita and Meyerhof (1967).

Table 3.3: Comparison of I_ρ values from Ueshita and Meyerhof (1967) and from the present study

H_1/a	$E_1/E_2=2$		$E_1/E_2=5$		$E_1/E_2=20$		$E_1/E_2=100$		$E_1/E_2=0.2$	
	Ueshita & Meyerhof	FE solution	Ueshita & Meyerhof	FE solution	Ueshita & Meyerhof	FE solution	Ueshita & Meyerhof	FE solution	Ueshita & Meyerhof	Steinbrenner's approach
0.5	0.669	0.679	0.6	0.608	0.474	0.469	0.307	0.304	1.013	1.048
1.0	0.619	0.570	0.451	0.435	0.281	0.279	0.171	0.157	1.682	1.613
2.0	0.513	0.480	0.313	0.293	0.170	0.151	0.092	0.072	2.595	2.390
3.0	0.465	0.430	0.255	0.236	0.128	0.106	0.065	0.044	3.086	2.784

2. Kay and Cavagnaro (1983) conducted site borings in Adelaide, South Australia, for soil identification and for performing down-hole plate load (DHPL) test to obtain drained Young's modulus, E' . Figure 3.9 shows the soil profile and plot of E' values with depth. This building rested on a raft of dimensions 33.5 m x 39.5 m placed at a depth of about 4m from the ground surface. Based on the variation of E' with depth, the soil profile below the raft can be assumed to consist of two finite layers of thickness equal to 2 m and 8 m with E' equal to 44 MPa and 60 MPa, respectively, and overlying a very stiff layer. Settlement measured at this site ranged between 16-18mm for applied load of 134 kPa. The settlement of the building using the method proposed in this study was compared with the observed settlement at the site.

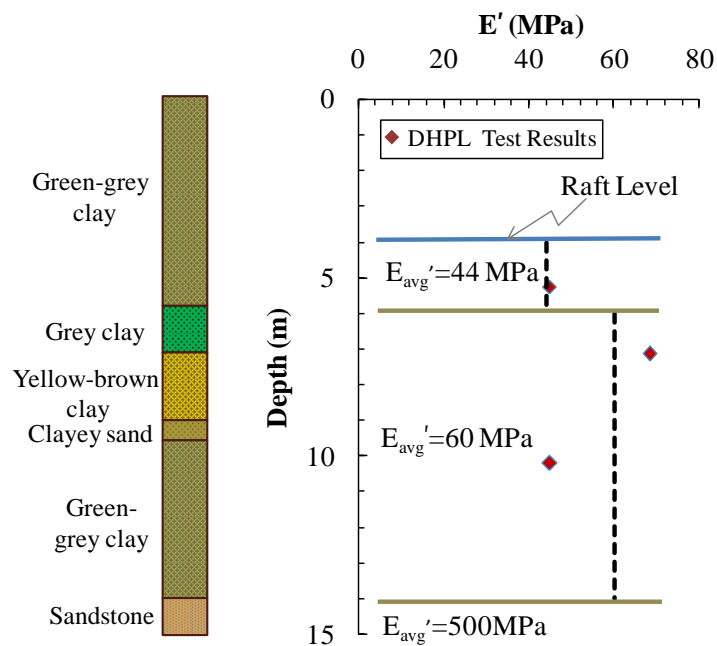


Figure 3.9: Soil profile with the variation of E' with depth at Savings Bank Building in the City of Adelaide, South Australia (Kay and Cavagnaro, 1983)

In order to use the charts proposed in this paper, an equivalent circular area of radius equal to 20 m corresponding to the raft area was obtained. Using the notation of Eq. [3.2], $q=134$ kPa, $H_1=2$ m, $H_2=8$ m, $a=20$ m and $H_1/a=0.1$, $H_2/a=0.4$, $E_1=44$ MPa, $E_2=60$ MPa. For the stiff clays of the Adelaide area, $\nu=0.2$ is appropriate (Kay and Cavagnaro [1983]). The corresponding settlement from the proposed Steinbrenner's method (Eq. [3.2]) gives settlement at the center of the raft equal to 19 mm which is in good agreement with the measured settlement values of 16-to18 mm. The slight difference might be due to [a] replacement of loading on raft with load on an equivalent circular area and [b] neglecting the top 4m overburden above the raft level.

3.2 Load on a Rigid footing

3.2.1 Elastic solution

Vesic's chart can be used to obtain the vertical displacement influence factors due to load applied on the rigid footing as shown in Fig. 3.10. For a multi-layered system of n layers, equation for the settlement, $\rho_z|_n$ at the center is given by Eq. [3.1] & [3.2].

A model problem with rigid footing (simulated by providing uniform prescribed displacement below the footing) for a uniform elastic medium of $H=4\text{m}$, $E=1000\text{kPa}$ and $\nu=0.33$ was solved in finite element solution (Plaxis 2D 8.2 version). The displacement obtained was 1.03m for contact pressure of 1000 kPa from the elastic solution, whereas the displacement obtained from Vesic's chart for the same problem is 1.01m , a difference of about 2.9% in comparison with the Finite element model.

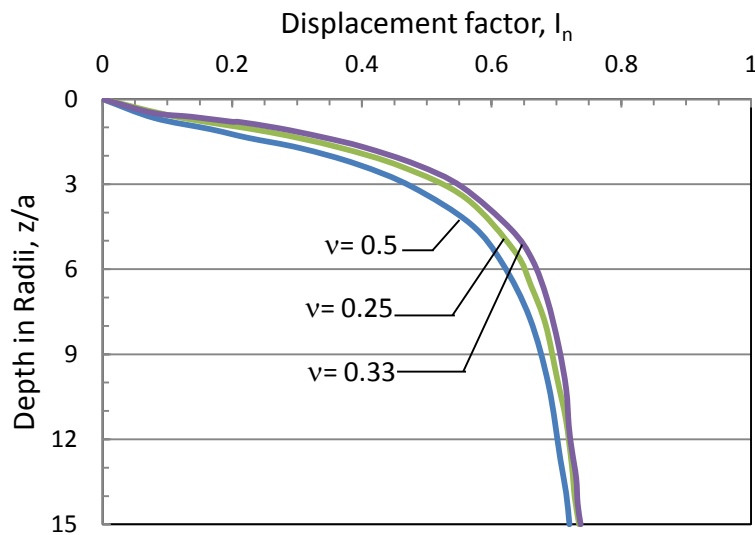


Figure 3.10: Displacement factors for layered systems for load on rigid footing (modified after Vesic [1963])

3.2.2 Finite element solution

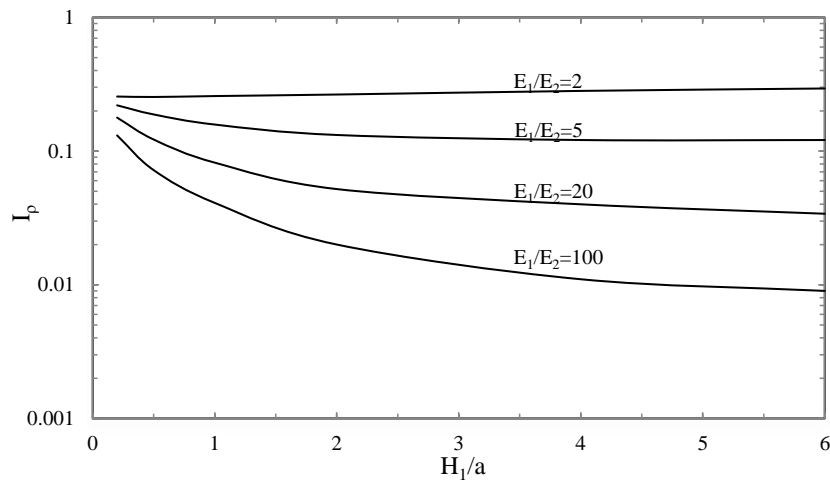
Figure 3.11 show the variations of I_ρ with H_1/a , for $E_1/E_2=2$ -to-100 and $\nu_1=\nu_2=0.35$ based on finite element solution.

Figure 3.11a shows that as the thickness of the top stiff layer increases, the settlement of the two-layer system decreases from $E_1/E_2=2$ -100. For $E_1/E_2=2$, I_ρ value is almost constant for H_1/a from 0.2-to-6.0. For the cases $E_1/E_2=5, 20, 100$ the rate of decrease of I_ρ with H_1/a is higher for relatively low H_1/a than for high H_1/a values. This decrease increases with

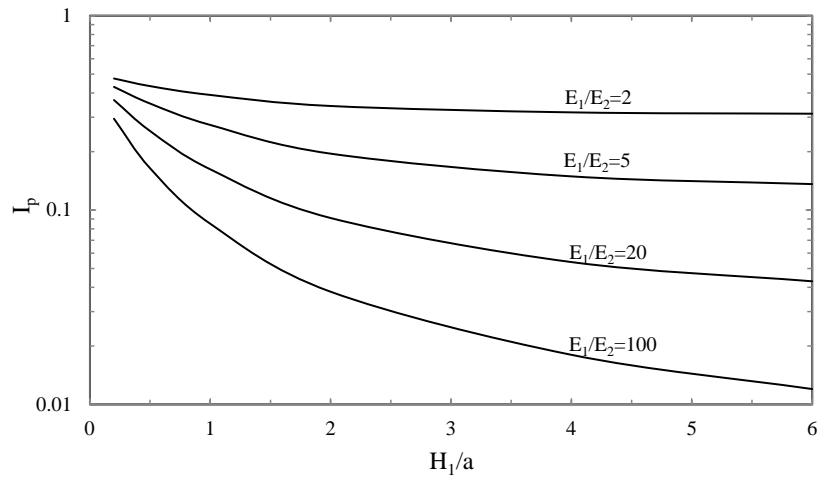
increase in E_1/E_2 values. For instance, I_ρ decreases by 72.2% as H_1/a increases from 0.5-to-2.0 for $E_1/E_2=100$, whereas it is only decreases by 29.7% for the same increase in H_1/a (0.5-to-2.0m) for $E_1/E_2=5$.

Similar trend is observed for the case of $H_2/a=4$ as shown in Fig. 3.11b. The rate of decrease with H_1/a is more for $H_2/a=4$ than that of the $H_2/a=1$. For instance, I_ρ decreases by about 72% for $H_2/a=1$ and it is decreases by about 76% for $H_2/a=4$ as H_1/a increases from 0.5-to-2.0 for $E_1/E_2=100$.

Figure 3.12 shows the comparison of flexible footing and rigid footing with respect to the variation of I_ρ with H_1/a from Finite element solutions for $\nu_1=\nu_2=0.35$, $E_1/E_2=2-100$, $H_2/a=4$. I_ρ values for rigid footing are found to be less than that for flexible footing. The ratio of rigid footing I_ρ to flexible footing I_ρ are 0.685, 0.645, 0.587, and 0.573 for $E_1/E_2=2, 5, 20$ and 100, respectively, at $H_1/a= 0.2$. As H_1/a increases from 0.2-6.0, the ratio of rigid footing I_ρ to flexible footing I_ρ increases gradually. For instance, the ratio of rigid footing I_ρ to flexible footing I_ρ are 0.747, 0.755, 0.811, 0.857 for $E_1/E_2=2, 5, 20$, and 100 respectively at $H_1/a=6.0$.



(a) $H_2/a=1$



(b) $H_2/a=4$

Figure 3.11: Variation of I_p with H_1/a from Finite element solutions for $\nu_1=\nu_2=0.35$, $E_1/E_2=2-100$

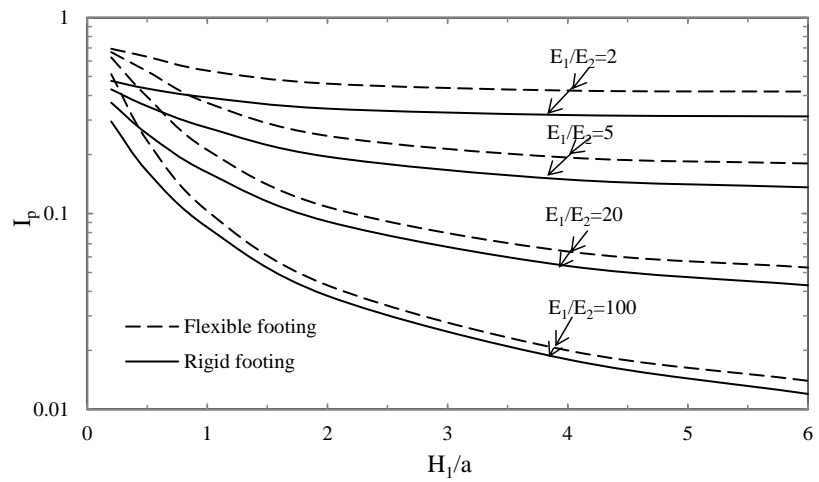


Figure 3.12: Comparison of flexible footing and rigid footing for variation of I_p with H_1/a from finite element solutions for $\nu_1=\nu_2=0.35$, $E_1/E_2=2-100$, $H_2/a=4$

Chapter 4

Load-settlement response of finite two-layer system using Mohr-Coulomb model

Linear stress-strain model can be used only when the loads are within elastic regime. In this Chapter, linear elastic-perfectly plastic model (Figure 4.1) is considered for the layered soil system to estimate the settlements due to circular load acting on both flexible and rigid footings resting on finite two-layer system. Mohr-Coulomb model is used as a first approximation of soil behavior.

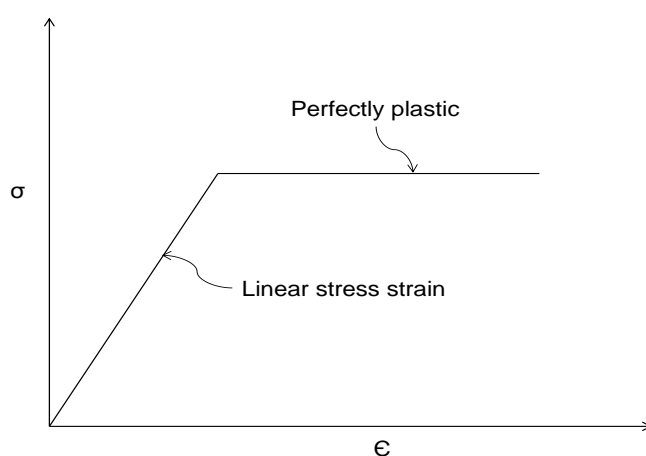


Figure 4.1: Elastic perfectly plastic behavior of soil under external load

Additional parameters - cohesion (c), friction angle (Φ), dilatancy angle (Ψ) are required other than elastic parameters for elasto-plastic behavior of soil. For the present case, cohesion of the soil is taken as 0° with no dilatancy ($\Psi=0^\circ$). Angle of shearing resistance of the top layer is taken as 36° (considering a strong top layer of medium dense sand) and for bottom layer it is taken as 32° (considering a weak bottom layer of loose sand). Typical soil model parameters used in the study

using Mohr Coulomb model (elastic- perfectly plastic) for circular loading on finite two-layered soil profile is shown in Fig. [4.2].

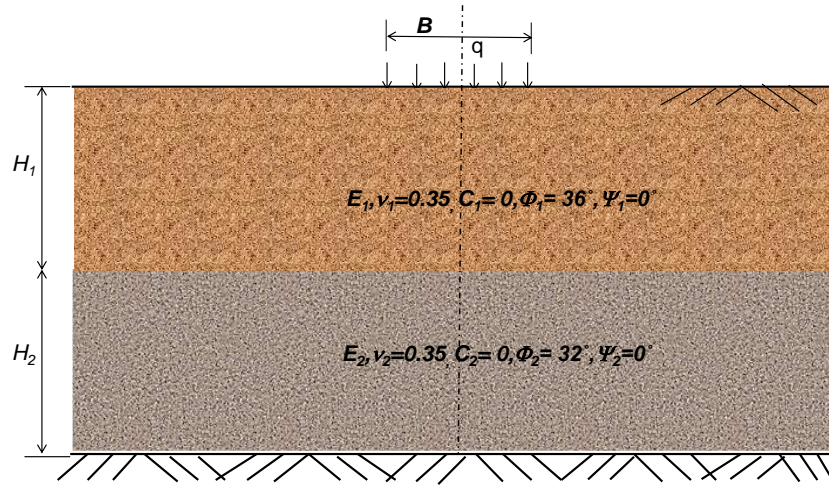


Figure 4.2: Mohr-Coulomb model for load on finite two-layered soil profile.

4.1 Load on a Flexible footing

Analytical solutions are not available to calculate the settlements of finite two-layered soil profile considering non-linear analysis. These settlements are predicted using PLAXIS 2D. The displacement influence factor I_ρ is obtained by equating the settlement of two-layer system $\rho_z|_2$ to qBI_ρ/E_2 as shown in Eq. [4.1].

$$i.e., \rho_z|_2 = \frac{qB}{E_2} I_\rho$$

$$\Rightarrow I_\rho = \frac{\rho_z|_2 E_2}{qB} \quad [4.1]$$

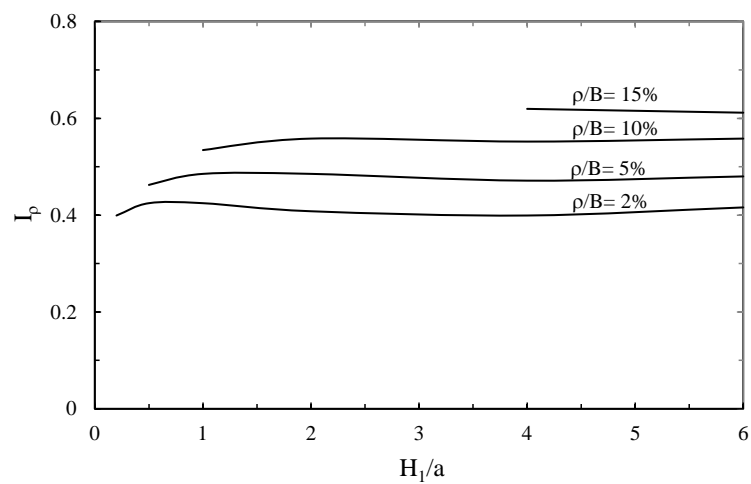
The vertical displacement factor I_ρ for the two-layer system is proposed for various values of $H_1/a = 0.1$ -to- 6.0 , $H_2/a = 1$ and 4 , $E_1=2000kPa$, $E_2=1000kPa$, $\nu_1=\nu_2=0.35$.

Figure 4.3 shows the variations of I_ρ with H_1/a , for $E_1=2000kPa$, $E_2=1000 kPa$, $\nu_1=\nu_2=0.35$, $H_2/a = 1$ and 4 , respectively, for ρ/B values in the range 2%-15% based on finite element solution. Loading is applied on the footing till the respective ρ/B values are attained.

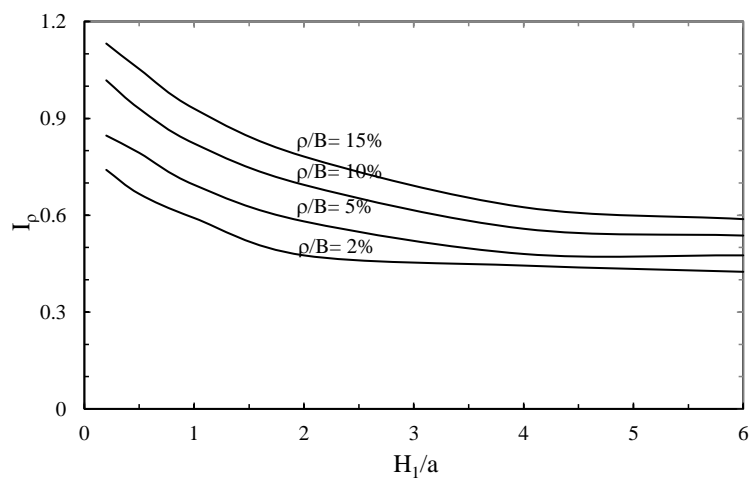
Figure 4.3a shows that for relatively thin bottom layer ($H_2/a=1.0$), the effect of the thickness of the top stiff layer on the settlement of the two-layer system is insignificant. For some cases, the soil

system collapse before the prescribed ρ/B values are reached. Hence, the data points corresponding to such ρ/B values are not shown in the plot.

Figure 4.3b shows that as the thickness of the top stiff layer increases, the settlement of the two-layer system decreases. The rate of decrease increases with increase in ρ/B values. The rate of decrease of I_ρ with H_1/a is higher for relatively low H_1/a (till $H_1/a = 3.0$) than for high H_1/a values. For instance, I_ρ decreases by 10% as H_1/a increases from 0.2-to-0.5, whereas it decreases only by 4% for increase in H_1/a from 4.0-to-6.0 for $\rho/B = 2\%$. For this case, soil body did not collapse before reaching ρ/B value due to the large bottom layer thickness ($H_2/a=4$).



(a) $H_2/a=1$



(b) $H_2/a=4$

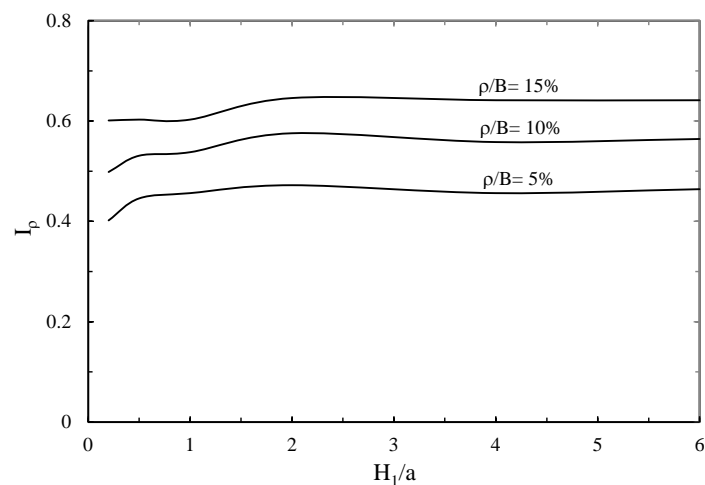
Figure 4.3: Variation of I_ρ with H_1/a from Finite element solutions for $\nu_1=\nu_2=0.35$, $E_1=2000kPa$, $E_2=1000kPa$

4.2 Load on a Rigid footing

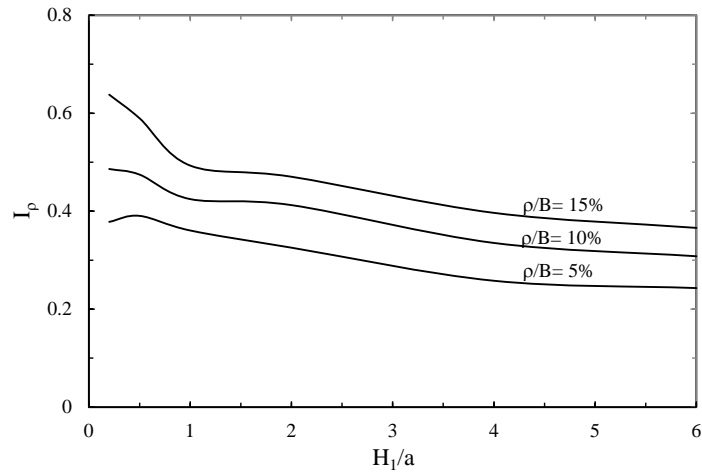
q is taken as average contact pressure instead of uniform pressure from the Eq. [4.1] for calculating the displacement influence factors(I_ρ) for load on rigid footing.

Figure 4.4 and Figure 4.5 show the variations of I_ρ with H_1/a , for $E_2=1000 \text{ kPa}$, $E_1=2000 \text{ kPa}$, 5000 kPa , 20000 kPa and $\nu_1=\nu_2=0.35$, $H_2/a = 1$ and 4 , respectively, for ρ/B values in the range 2%-15% based on finite element solutions.

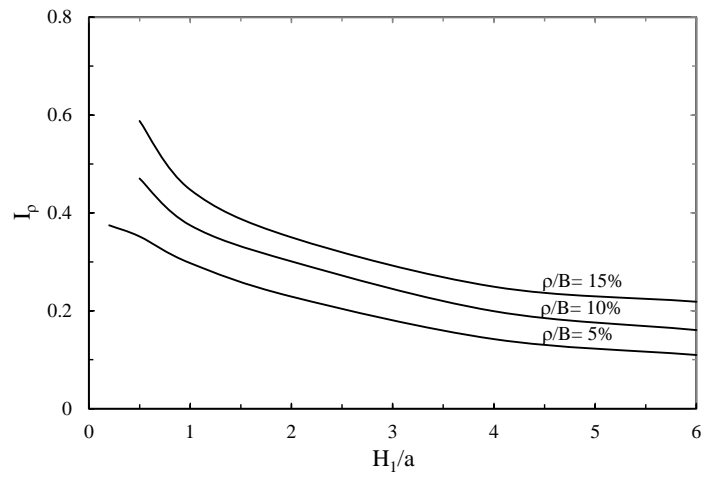
Figure 4.4a shows that as the thickness of the top stiff layer increases, the settlement of the two-layer system is more or less constant, similar behavior as was noticed for flexible footing. Figure 4.4b shows that as the thickness of the top stiff layer increases, the settlement of the two-layer system decreases due to increase in top layer stiffness. The rate of decrease of I_ρ with H_1/a is higher for relatively low H_1/a than for high H_1/a values. For instance, I_ρ decreases by 7% as H_1/a increases from 0.5-to-0.1, whereas it is only decreases by 5% for increase in H_1/a from 4.0-to-6.0 for $\rho/B= 2\%$. Similar trend is observed for $E_1=20000 \text{ kPa}$ as shown in Fig. 4.3c. But the rate of decrease of I_ρ with H_1/a is more for $E_1=20000 \text{ kPa}$ than that of $E_1=5000 \text{ kPa}$. For instance, I_ρ decreases by 7% for $E_1=5000 \text{ kPa}$, whereas it decreases by 15% for $E_1=20000 \text{ kPa}$ as H_1/a increases from 0.5-to-0.1.



(a) $E_1=2000 \text{ kPa}$



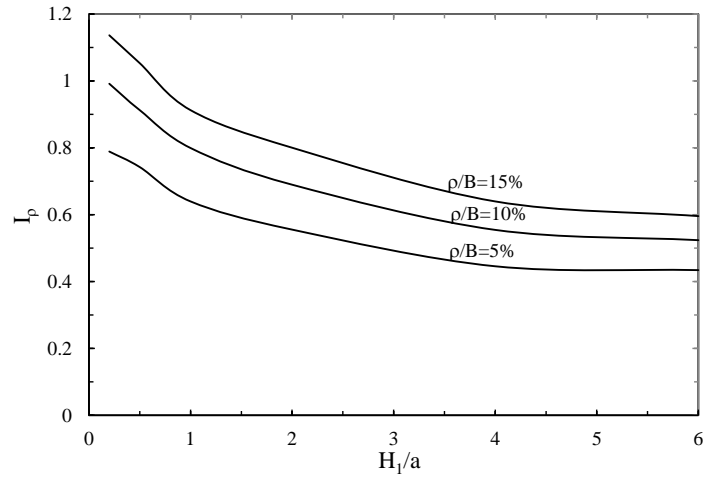
(b) $E_I=5000 \text{ kPa}$



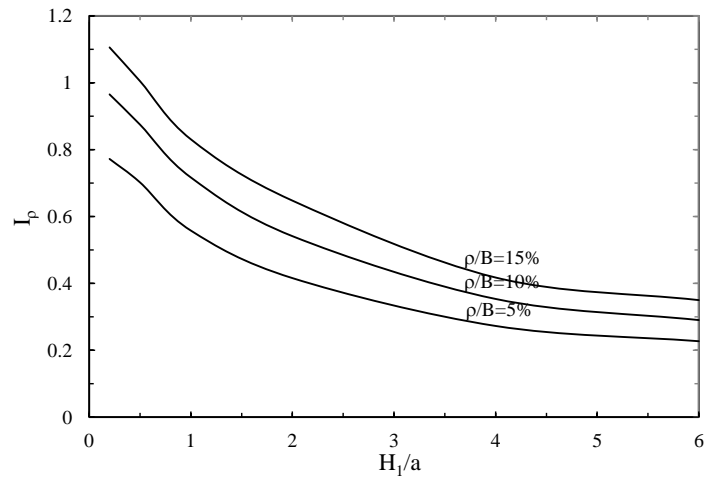
(c) $E_I=20000 \text{ kPa}$

Figure 4.4: Variation of I_ρ with H_1/a from Finite element solutions for $\nu_1=\nu_2=0.35$, $E_2=1000 \text{ kPa}$, $E_I=2000 \text{ kPa}$, 5000 kPa , 20000 kPa respectively corresponding to $H_2/a=1$

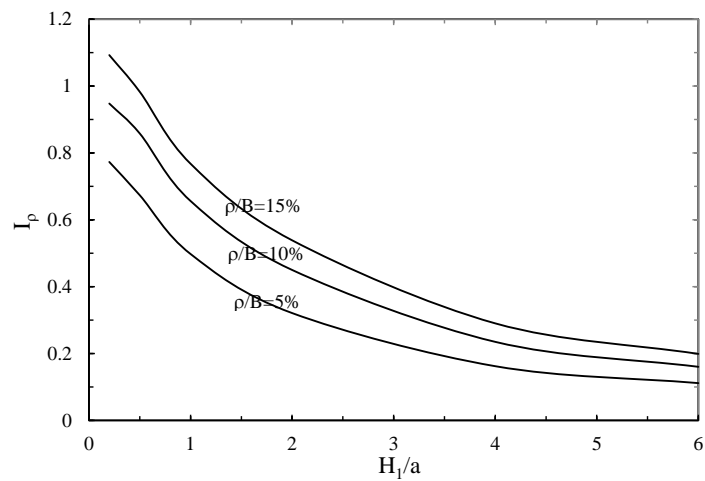
Figure 4.5a shows that as the thickness of the top stiff layer increases, the settlement of the two-layer system decreases. The rate of decrease of I_ρ with H_1/a is higher for relatively low H_1/a than for high H_1/a values. For instance the rate of decrease I_ρ value is decreases by 5% with H_1/a values from 0.2-to 0.5 and it is decreases by 2% with H_1/a values from 4.0-to 6.0 for $\rho/B=5\%$. Similar trend is observed for $E_I=5000 \text{ kPa}$ and 20000 kPa as shown in Fig. 4.5b and Fig. 4.5c, respectively. But the rate of decrease of I_ρ with H_1/a is more for larger top layer stiffness. For instance, I_ρ decreases by 5% for $E_I=2000 \text{ kPa}$, 9% for $E_I=5000 \text{ kPa}$ and 13% for $E_I=20000 \text{ kPa}$ as H_1/a increases from 0.2-to-0.5.



(a) $E_I=2000kPa$



(b) $E_I=5000kPa$



(c) $E_I=20000kPa$

Figure 4.5: Variation of I_p with H_1/a from Finite element solutions for $\nu_1=\nu_2=0.35$, $E_2=1000 kPa$, $E_I=2000 kPa$, $5000 kPa$, $20000 kPa$ respectively corresponding to $H_2/a=4.0$

Figure 4.6 shows that Comparison of flexible footing (Ff) and rigid footing (Rf) for variation of I_ρ with H_1/a from Mohr-Coulomb model using finite element solutions for $\nu_1=\nu_2=0.35$, $E_1=2000kPa$, $E_2=1000kPa$ and $H_2/a=4$. Ratio of rigid footing I_ρ to flexible footing I_ρ are 0.931, 0.974 and 1.0 for $\rho/B=5\%$, $\rho/B=10\%$ and $\rho/B=15\%$, respectively, at $H_1/a=0.2$. With increase in ρ/B values, this ratio increases and becomes 1.0 at $H_1/a=0.2$ for $\rho/B=15\%$, indicating that the rigid footing I_ρ is equal to flexible footing I_ρ .

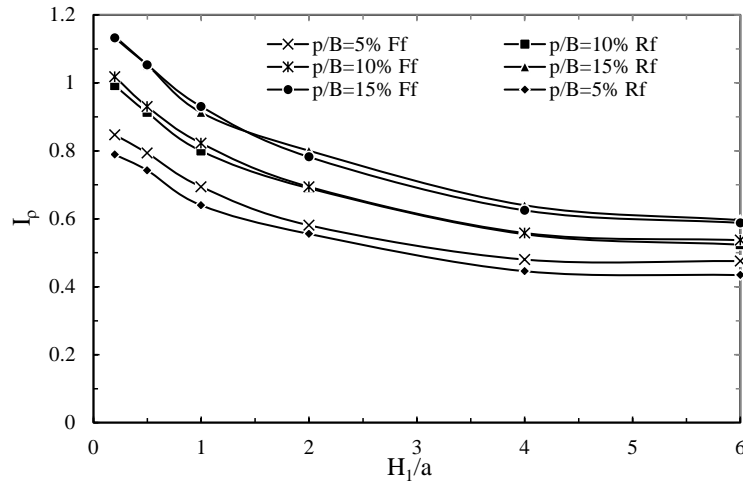


Figure 4.6: Comparison of flexible footing (Ff) and rigid footing (Rf) for variation of I_ρ with H_1/a from Mohr-Coulomb FE solutions for $\nu_1=\nu_2=0.35$, $E_1=2000kPa$, $E_2=1000kPa$ $H_2/a=4$

Chapter 5

Conclusions

5.1 Elastic analysis due to flexible load on finite two-layer system

Displacement factors were proposed to estimate settlements due to uniform circular load acting flexible footing resting on a finite two-layer system for a soft layer overlying a stiff layer ($E_1/E_2 < 1.0$) and a stiff layer overlying a soft layer ($E_1/E_2 > 1.0$). For a soft layer overlying a stiff deposit ($E_1/E_2 < 1.0$), displacement factors obtained from Steinbrenner method are found to compare well with the results from the Finite element solution. Steinbrenner's method provides a good approximation for the settlements for the two-layer system with $E_1/E_2 < 1.0$. Settlement influence factors for the finite two-layer profile for E_1/E_2 are newly provided in this thesis. The displacement factors proposed in this study using Steinbrenner and Finite element methods are in good agreement with the factors proposed by Ueshita and Meyerhof.

5.1.1 Bottom layer is stiffer than the top layer

[1] As the thickness of the top layer increases, the settlement of the two-layer system increases for $E_1/E_2 = 0.5-0.01$. The rate of increase of I_ρ with H_1/a is higher for relatively low H_1/a than for high H_1/a values. This increase increases with increase in E_1/E_2 values.

[2] As the thickness of the bottom layer increases, the settlement of the two-layer system increases for $E_1/E_2 = 0.1-0.01$ for smaller top layer thickness, and it is almost constant for higher top layer thickness.

5.1.2 Top layer is stiffer than the bottom layer

[1] As the thickness of the top layer increases, the settlement of the two-layer system decreases for $E_1/E_2 = 2-100$. The rate of decrease of I_ρ with H_1/a is higher for relatively low H_1/a than for high H_1/a values. This decrease increases with increase in E_1/E_2 values.

[2] As the thickness of the bottom layer increases, the settlement of the two-layer system increases for $E_1/E_2= 2-100$. The rate of increase of I_ρ with H_2/a is higher for larger E_1/E_2 ratios compared to that of lower E_1/E_2 ratios.

5.2 Elastic analysis due to rigid load on finite two-layer system

[1] As the thickness of the top layer increases, the settlement behavior is similar to that of the flexible loading for the case of $E_1/E_2 > 1$.

[2] The ratio of rigid footing I_ρ to flexible footing I_ρ is initially less than $\pi/4$ at lower H_1/a value, and then increases gradually with H_1/a and becomes $\pi/4$ at higher H_1/a value.

5.3 Nonlinear analysis due to flexible load on finite two-layer system

[1] For H_2/a value equal to 1.0, effect of H_1/a on I_ρ is insignificant for the top layer stiffness is greater than the bottom layer.

[2] For H_2/a value equal to 4.0, I_ρ values decrease with increase in H_1/a . The rate of decrease of I_ρ with H_1/a is higher for relatively low H_1/a (till $H_1/a = 3.0$) than for high H_1/a values.

5.4 Nonlinear analysis due to rigid load on finite two-layer system

[1] I_ρ values decrease with increase in H_1/a . The rate of decrease of I_ρ with H_1/a is higher for relatively low H_1/a (till $H_1/a = 3.0$) than for high H_1/a values when the top layer stiffness is greater than the bottom layer.

[2] I_ρ values decrease with increase in the top layer stiffness for a given bottom layer stiffness. The rate of decrease of I_ρ with H_1/a is higher for relatively higher E_1 values than for lower E_1 values for constant bottom layer stiffness.

[3] The rate of decrease of I_ρ with H_1/a is more for the H_2/a equal to 4.0 than that of H_2/a equal to 1.0.

[4] The ratio of rigid footing I_ρ to flexible footing I_ρ is initially less than 1.0 for $\rho/B=5\%$, and it increases with ρ/B and reaches 1.0 for $\rho/B=15\%$, (0.3m). The effect of H_1/a on this ratio is insignificant.

References

- [1] Ahlvin, R.G., and Ulery, H.H. (1962). Tabulated values for determining the complete pattern of stresses, strains, and deflections beneath a uniform load on a homogenous half space. Highway Research Board, Bulletin 342, pp. 1-13.
- [2] Anbazghan and Sitharam (2006). Evaluation of Dynamic Properties and Ground Profiles using MASW, 13th Symposium on Earthquake Engineering, Indian Institute of Technology, Roorkee, Paper No. 008.
- [3] Burmister, D.M. (1962). Application of layered system concepts and principles to interpretations and evaluations of asphalt pavement performances and to design and construction. Proc. International on Structural Design of Pavements, Univ. of Michigan, pp. 441-453.
- [4] Kay, J. N., Cavagnaro, R. L. (1983). Settlement of raft foundations. Journal of Geotechnical Engineering, Vol. 109, No. 11, pp. 1367-1382.
- [5] L. M. Zhang and S. M. Dasaka (2010). Uncertainties in Geological Profiles versus Variability in Pile Founding Depth. Journal of Geotechnical and Geoenvironmental Engineering, ASCE, Vol. 136, No. 11, pp. 1475-1488.
- [6] Palmer, L.A. and Barber, E.S., 1940. Soil displacement under a circular loaded area. Proc. Highway Research Board, Vol. 20, pp. 279-286.
- [7] Poulos, H; and Davis, E. H. Elastic Solutions for Soil and Rock Mechanics.
- [8] Poulos, H.G., 1968[a]. The behavior of rigid circular plate resting on a finite elastic layer. Civil. Engg. Trans., Instn. Engrs., Aust., Vol. CE10, pp. 213-219.
- [9] R.B.J. Brinkgreve & W. Broere and D. Waterman, Plaxis 2D-version 9.0, Delft university of technology and Plaxis b.v., The Netherlands.
- [10] R.F. Craig, Craig's Soil Mechanics. Seventh edition, Taylor and Francis Group, London and New York.
- [11] Sneddon, I.N., 1946. Boussinesq's problem for flat ended cylinder. Proc. Cambridge philosophy society., Vol. 42, pt. 1, pp. 29-39.
- [12] Ueshita, K. and Meyerhof, G.G., 1967. Deflection of multilayer soil systems. Journal of Soil Mechanics and Foundations Division, ASCE, No. SM5, pp. 257-282.
- [13] Vesic, A.S., 1963. Discussion, Session III, Proc. 1st International Conference on Structural Design of Asphalt Pavements, Univ. of Michigan, pp. 283-290.
- [14] Yang H. Huang, Pavement Analysis and Design. Second Edition, New Jersey, USA.